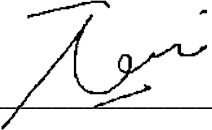


APPROVAL SHEET

This dissertation/thesis entitled “**ASSESSMENT OF POTENTIAL CLIMATE HAZARDS IN KUALA KRAI, KELANTAN USING STATISTICALLY DOWNSCALED REGIONAL CLIMATE MODEL**” was prepared by NGU JUN JIE and submitted as partial fulfillment of the requirements for the degree of Master of **Environmental Technology** / Doctor of Philosophy in _____ at Universiti Tunku Abdul Rahman.

Approved by:



(ChM. Ts. Dr. Tan Kok Weng)

Date: 20/12/2021

Professor/Supervisor

Department of Environmental Engineering

Faculty of Engineering and Green Technology

Universiti Tunku Abdul Rahman

**FACULTY OF ENGINEERING AND GREEN
TECHNOLOGY**

UNIVERSITI TUNKU ABDUL RAHMAN

Date: 20 December 2021

SUBMISSION OF DISSERTATION / THESIS*

It is hereby certified that **NGU JUN JIE** (ID No: **2100801**) has completed this dissertation / thesis* entitled “ **Assessment of Potential Climate Hazards in Kuala Krai, Kelantan Using Statistically Downscaled Regional Climate Model** ” under the supervision of **ChM. Ts. Dr. Tan Kok Weng** from the Department of **Environmental Engineering**, Faculty of **Engineering and Green Technology**.

I understand that the University will upload softcopy of my dissertation / thesis* in pdf format into UTAR Institutional Repository, which may be made accessible to UTAR community and public.

Yours truly,

ngu jun jie

(Ngu Jun Jie)

DECLARATION

I NGU JUN JIE hereby declare that the dissertation/thesis is based on my original work except for quotations and citations which have been duly acknowledged. I also declare that it has not been previously or concurrently submitted for any other degree at UTAR or other institutions.

NGU JUN JIE

(NGU JUN JIE)

Date 20 December 2021

**Assessment of Potential Climate Hazards in Kuala Krai,
Kelantan Using Statistically Downscaled Regional Climate
Model**

By

NGU JUN JIE

A thesis submitted to the Faculty of Engineering and Green
Technology,

University Tunku Abdul Rahman,

in partial fulfillment of the requirements for the degree of

Master of Environmental Technology

November 2021

ABSTRACT

Assessment of Potential Climate Hazards in Kuala Krai, Kelantan Using Statistically Downscaled Regional Climate Model

Ngu Jun Jie

In Peninsular Malaysia, Kelantan is one of the black spot of flood and the rainfall being highly concerned. Therefore, historical rainfall pattern in Kelantan is worth to study and study of the local rainfall pattern in the future is significant to the disaster preparation. In this thesis paper, future precipitation was modelled based on RCP4.5 and RCP8.5 predictors obtained from CanESM2. After obtaining all the data, calibration of the model was carried out by using the SDSM4.2 software that including screening process. In order to determine the reliability of the model, several statistical tests were implemented for model validation. For statistical test of the model, both Pearson correlation analysis and linear regression test indicated that RCP4.5 could simulate the rainfall pattern slightly better than RCP8.5. Although future rainfall prediction is mainly depending on RCP4.5, since both are likely reliable, the rainfall prediction under RCP8.5 was carried out as a potential alternative in the future as well. Based on the outcome, the potential of future flood are only 2 days within next 80 years under RCP4.5 while 7 days within next 80 years under RCP8.5. Therefore, majority of the future precipitation events will not induce severe flood events until the end of 2100.

LIST OF TABLES

Table	Page
1. Sources of CO ₂ in construction (Adesina, 2020).	4
2. The influence of elevated temperature on the wheat yields (Araya, 2020).	5
3. Classification of RCPs.	8
4. The performance of models under 6 variables (Xuan et al., 2017).	8
5. Characteristic of dynamical and statistical downscaling approaches (Roux et al., 2017; Kotamarthi et al., 2016; Gutmann et al., 2012; Sunyer et al., 2012; Boe et al., 2007). Error! Bookmark not defined.	
6. Test duration of modeling for Addis Ababa and Entoto stations (Feyissa et al., 2018).	12
7. The result of model calibration and validation (Feyissa et al., 2018).	12
8. Temperature and precipitation with various scenarios from downscaled modelling (Feyissa et al., 2018).	13
9. Details of the selected hydrometric stations at the Langat River Basin (Soh et al., 2018).	14
10. Drought classification (Huang et al., 2016).	16
11. Summary statistic of indices (Huang et al., 2016).	17
12. The selected station.	19
13. The 26 predictors from CanESM2.	21
14. Description for ρ .	25
15. The reduced mean and reduced standard deviation in Gumbel's extreme value distribution (source: https://uomustansiriyah.edu.iq/media/lectures/5/5_2019_04_22!08_22_05_PM.pdf) .	26
16. Five individual rainfall data in the flood events.	27
17. Reliability test between RCP4.5 and RCP8.5.	32

18. Historical flood events happened in Kuala Krai.	33
19. Rainfall intensity of historical flood events.	33
20. Peak daily rainfall under RCP4.5	34
21. Peak daily rainfall under RCP8.5	35
22. Numbers of projects approved in Gua Musang, Kuala Krai and Tanah Merah (Samsurijan et al., 2018).	37

LIST OF FIGURES

Figure	Page
1. The location of Kuala Krai district (Nayan et al, 2017).	3
2. The river flow of the Kelantan River (Hamid, 2018).	3
3. Carbon contain in building component (Hammond and Jones, 2008).	4
4. Performances of 4 models under a) multi-years average simulated precipitation. b) multi-years average monthly precipitation. c) multi-years average seasonal precipitation. d) multi-years average annual maximum 1-day precipitation. e) multi-years average annual maximum precipitation in 5-days consecutively (Gao et al., 2020).	9
5. The location of meteorological stations in Langat River Basin, Malaysia (Soh et al., 2018).	14
6. Plotting of SPEI with 1-month interval (Soh et al., 2018).	15
7. Plotting of SPEI with 3-month intervals (Soh et al., 2018).	15
8. Plotting of SPEI with 6-month intervals (Soh et al., 2018).	16
9. SEP, SPI-1, SPI-6, SPI-12 and EDI plotting for comparison a)2016-2040, b)2041-2070, c)2071-2100 (Huang et al. ,2016).	17
10. Seasonal changes for 2071-2100 at three stations (Hussain et al, 2017).	18
11. SDSM software.	19
12. Work flow chart.	20
13. The CanESM2 predictors represents climate parameters for this cell covered region.	21
14. Data screening for lag function -3.	23
15. Precipitation model with lag function -3.	28
16. Tmax model with lag function -3.	28
17. Tmin model with lag function -3.	29

18. Probability Density Function of Tmin January 2006 to December 2013.	29
19. Probability Density Function of Tmax January 2006 to December 2013.	30
20. Estimation of future temperature.	30
21. Probability Density Function of precipitation January 2006 to May 2019	31
22. Estimation of future precipitation under RCP4.5.	32
23. Return period of historical flood.	35
24. Return period under RCP4.5.	36
25. Return period under RCP8.5.	Error! Bookmark not defined. 6

LIST OF ABBREVIATIONS

Tmax	Maximum temperature
Tmin	Minimum temperature
GCM	Global climate model
RCP4.5	Representative Concentration Pathways 4.5
RCP8.5	Representative Concentration Pathways 8.5
IPCC	Intergovernmental Panel on Climate Change
ECP	Extended Concentration Pathways
CMIP5	Coupled Model Intercomparison Project Phase 5
SRES	Special Report Emission Scenarios
SPEI	Standardized Precipitation Evapotranspiration Index
WAAN	Wavelet-ARIMA-ANN model
CanESM2	Second Generation Canadian Earth System Model
NCEP	National Central of Environmental Prediction
SPI	Standard Precipitation Index

CCCma	Canadian Centre for Climate Modelling and Analysis
MST	Mean sum of squares
MSE	Mean sum of squares
ρ	Spearman's correlation
r^2	Coefficient of determination
r_value	Pearson correlation
P_t	Desired hourly rainfall
P_{24}	24-hours rainfall data
t	Final rainfall duration
Y_n	Reduced mean in Gumbel's extreme value distribution
S_n	Reduced standard deviation in Gumbel's extreme value distribution
K_t	Frequency factor
PDF	Probability Density Function

TABLE OF CONTENTS

	Page
ABSTRACT	i
LIST OF TABLES	ii
LIST OF FIGURES	iv
LIST OF ABBREVIATIONS	vi
CHAPTER	
1.0 INTRODUCTION	1
1.1 Overview	1
1.2 Problem statement	1
1.3 Scope of study	2
2.0 LITERATURE REVIEW	4
2.1 Climate change	4
2.1.1 Causes	5
2.1.2 Impact	5
2.2 Climate modeling	6
2.2.1 The General Circulation Models	7
2.3 Regional Climate Model	9
2.3.1 Dynamical downscaling	10
2.3.2 Statistical downscaling	10
2.4 Climate hazard	11
2.5 Past studies	11
3.0 MATERIALS AND METHODS	19
3.1 Workplan	19
3.2 CanESM2	21
3.2.1 Predictors screening	21
3.2.2 Model calibration	23

3.2.3	Model validation	23
3.2.4	Statistical analysis	24
3.3	Computation for flood return period	25
3.4	Determination of flood hazard threshold	27
4.0	DISCUSSION	28
4.1	Temperature model (RCP4.5 & RCP8.5)	28
4.2	Rainfall model (RCP4.5 & RCP8.5)	31
4.3	Potential flood risk analysis	33
5.0	CONCLUSION	38
5.1	Conclusion	38
5.2	Recommendation for further study	38

REFERENCES

CHAPTER 1

INTRODUCTION

1.1 Overview

In recent decades, various countries keep concerning about the anthropogenic climate change. Since the anthropogenic carbon emission is the main driver of the climate change, policies and regulations are proposed in order to cap and reduce the carbon footprint. The rising temperature will provide more heat energy into the water cycle and therefore the disasters are aggravated. Statistical downscaled regional climate model is a deterministic model that simulating future precipitation based on the historical station data. In order to determine the potential disaster, flood, modeling measurements are developed to simulate the future precipitation trend.

1.2 Problem statement

Climate change is referring to the global climate changes in long-term and it is one of the famous topics in recent decades. The climate is the usual weather in a region over a long period and it takes centuries or more to change. The weather can vary from time to time in terms of humidity, temperature, windiness, atmospheric pressure and cloudiness. The climate change could happen at its own naturally due to environmental factors but the climate change had been accelerated by human activity, which is also known as anthropogenic climate change. Due to the climate change, the melting glaciers is getting serious subsequently lead to the rising of sea levels and coast erosion. As one of the tropical countries, the rainfall is the main contributor to the river basin in Malaysia. With the influence of climate change, the annual rainfall intensity is varying and this issue can cause either the flood or drought events. In fact, there are a lot of studies regarding the influence of climate change has been done and various type of modeling are being proposed. Most of the time, it is difficult to construct a reliable modeling with the raw data given due to coarse resolution of the modeling. Therefore, downscaled modeling is needed to forecast for future changes. In this research, the Canadian climate model and the modeling software, Statistical Downscaling Model (SDSM), were utilized to calibrate model based on the precipitation data in Kuala Krai, Kelantan. The research is focusing on downscaling of an existing climate model and forecasting the rainfall intensity until 2100. On the other hand, the potential climate hazard could be determined with the outcome of downscaled model by using the flood threshold and return period.

Objectives

1. To develop Kuala Krai regional climate model using statistical downscaling method based on Representative Concentration Pathways (RCP) 4.5 and 8.5
2. To analyse the reliability of downscaled regional climate model using parametric statistical tests
3. To compute the flood return period using Gumble Distribution
4. To propose the potential flood risk of Kuala Krai based on regional climate model RCP scenario

1.3 Scope of study

In recent decades, the extreme climate event induced disaster occurs frequently and some pointed that it is the indirect impact of human activities. Plus, the climate change is one of the global issues that resulting a notable influence on the environment, which impact the aquaculture and agriculture field negatively (Rasul, 2021). Especially in Malaysia, the climate change could impact the economy growth of country indirectly because agriculture is one of the major incomes. As a result, the important of climate modeling is rising up as it can simulate the growth of current and future climate variation. A reliable climate model able to produce high accuracy data required such as temperature and rainfall intensity for further study in the hydrological modeling. Hence, there are a lot of studies being proposed to determine the consequences of anthropogenic activities on the climate change and study the impact of climate change on the environment. In fact, the return period of an extreme climate event and it is an effective measurement to predict the occurrence of disaster. With the influence of climate change, the rainfall amount become hardly to be predicted correctly. Therefore, the study of climate model could improve the accuracy of the outcome of hydrological model. In this research, the future precipitation in Kuala Krai River Basins in Kelantan, Figure 1, were simulated through both climate and hydrological modeling.

Kelantan river is the major water resource for the whole state which comprise of Bachok, Gua Musang, Jeli, Kota Bharu, Kuala Krai, Lojing, Machang, Pasir Mas, Pasir Puteh, Tanah Merah and Tumpat. This river merges with other two rivers, Galas and Lebir rivers, near the Kuala Krai and form a boarder downstream as shown in Figure 2. After meandering over the coastal plain, it will flow towards the South China Sea. Before 20th century, the Kuala Krai was a hilly tropical rain forest. Due to improvement in transportation link, the settlement starts growing and more and more agriculture activity can be found (Maruti *et al*, 2017). The total area of Kuala Krai is around 2329 km² and it is the most affected district during the massive flood in 2014 (Udin and Malek, 2018).

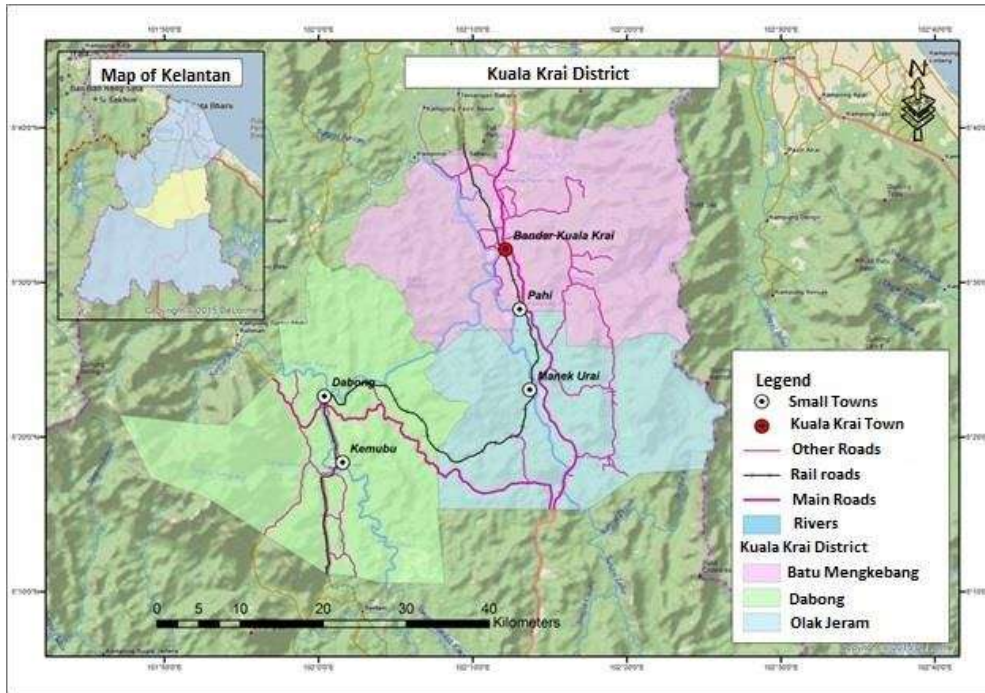


Figure 1 The location of Kuala Krai district (Nayan et al, 2017).



Figure 2 The river flow of the Kelantan River (Hamid, 2018).

CHAPTER 2

LITERATURE REVIEW

2.1 Climate change

2.1.1 Causes

The climate change always causes intensive climate hazard and it is related to the global warming. The global warming is the elevation in the average temperature of the atmospheric temperature gradually due to the increase in greenhouse gas amount. When the heat of sunlight enters the atmosphere, part of them will remain in the atmosphere and the other part will be radiated out into the space. The feature of absorbing and reradiating the heat store part of the energy radiated from Earth surface. Due to the presence of greenhouse gaseous, the earth surface is kept warm and it benefits the species live on the earth by radiating heat energy to the environment. A warmer atmosphere will result in raising sea level due to melting glaciers and more water evaporation could lead to more intensive climate hazard. For recent decades, the global warming usually refers to human induced climate change. Due to rapid development, the increase in emission of carbon dioxide has been proven that the main driver of global warming (Sohag et al., 2015). The carbon dioxide in the energy generation and the black carbon (soot) from incomplete combustion are contributing to the warming effect (Zheng et al, 2019; Kang et al, 2020; Schweizer, et at., 2020). Those black tiny particles are able to suspend into the atmosphere and warm the surrounding air with the absorbed heat energy. Besides, the burning of fossil fuel releases the carbon dioxide that sequestered underground and the carbon dioxide can trap heat more effective than soot. Based on Figure 3 and Table 1, the construction industry is also one of the sources of emission of CO₂.

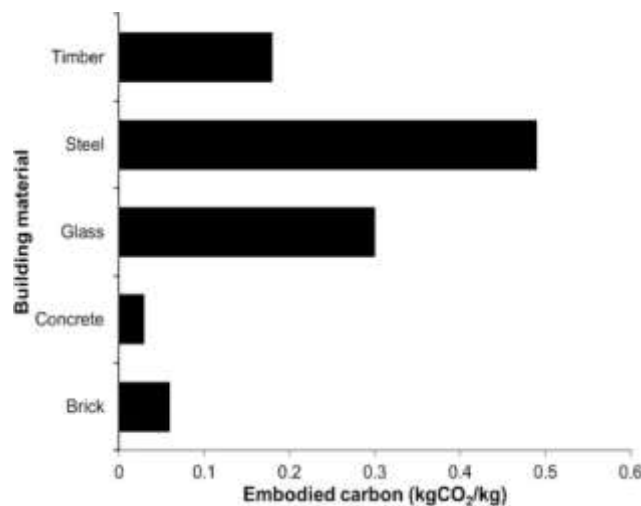


Figure 3 Carbon contain in building component (Hammond and Jones, 2008).

Table 1 Sources of CO₂ in construction (Adesina, 2020).

Source of carbon dioxide in concrete	Process
Raw materials	Mining

Concrete production

Processing
 Transportation
 Mixing
 Casting
 Transportation
 Compaction
 Curing

2.1.2 Impact

Other than sea level elevation and coastal erosion, based on (Keenan and Riley, 2018), it is found that there are 16.4% drop in the vegetation land area that has lower temperature and high-altitude ecosystem. The global warming could result in an unfavorable living condition for particular ecosystem and the reduction in producer yields in food chain. Some of the animal species could become extinct due to losing of habitat and food resources. Coral bleaching, the rising of oceanic temperature exceeds the tolerance threshold of corals result in thermal stress and subsequently expulse symbiotic zooxanthellae (Hussain and Ingole, 2020). The decline in coral leads to long-terms impacts on the eco-system and economic development. For examples, reduction in fishery production, economy impact on tourism industry or habitat variation. Besides, the global warming reduces the crop yield due to shorter growing period. Araya *et al* (2020) found that the days to maturity of wheat will be decreased for rising in temperature by 2 °C. From Table 2, the day to maturity in D. Markos and Adaba reduced by 10 % and 15 % respectively. If the temperature elevated by 1 °C, there will be 6% drop in the global wheat production (Zhao *et al.*, 2017). In history of Malaysia, there was a serious flood in December of 2014. As the result of the flood, the relocation of people causes the decline in economic development, the losses in crop yield and erosion of river bank (Yahara *et al.*, 2015).

Table 2 The influence of elevated temperature on the wheat yields (Araya, 2020).

Location	Baseline (1980–2005)			Climate change scenario					
	N (kg/ha)	Yield (kg/ha)	DM (days)	T (°C)	CO ₂ (μmol/mol)	Yield (kg/ha)	Changes (%)	DM (days)	Changes (%)
D. Markos	96	4530	92	2	380	4250	-6	84	-9
	128	5250	92	2	380	4652	-11	84	-10
	160	5660	93	2	380	5119	-10	84	-10
	96	4530	92	4	380	3740	-17	76	-17
	128	5250	92	4	380	4033	-23	76	-17
	160	5660	93	4	380	4312	-24	76	-18
	96	4530	92	2	571	4763	5	84	-9
	128	5250	92	2	571	5350	2	84	-10
	160	5660	93	2	571	5708	1	84	-10
	96	4530	92	4	571	4443	-2	76	-17
	128	5250	92	4	571	4856	-8	76	-17
	160	5660	93	4	571	5074	-10	76	-18
	96	4298	144	2	380	4120	-4	122	-15
	128	4898	145	2	380	4438	-9	123	-15
	Adaba	160	5218	145	2	380	4799	-8	124
96		4298	144	4	380	3635	-15	108	-25
128		4898	145	4	380	3579	-27	107	-26
160		5218	145	4	380	3854	-26	108	-25
96		4298	144	2	571	4826	12	122	-15
128		4898	145	2	571	5072	4	123	-15
160		5218	145	2	571	5386	3	124	-15
96		4298	144	4	571	4176	-3	108	-25
128		4898	145	4	571	4606	-6	107	-26
160		5218	145	4	571	4740	-9	108	-25

2.2 Climate modeling

The understanding towards the weather model always come before the climate model first. The weather models are always working at high resolution since it needs to generate the atmospheric data which cover a large area of region. Typically, the forecasted result has its own effective duration and it is around two-week maximum for the short timescales. Due to the behavior of weather that varying from time to time, there are few parameters, current atmospheric conditions and oceanic condition, are involving in the weather forecasting. Normally, the weather forecast will cover the local atmospheric variables such as temperature, humidity, wind speed, cloudiness or even air pressure. To come out with a reliable prediction, the meteorologists put more detailed variables that in finer resolution for model input to determine the weather for current or future. Based on these reliable atmospheric data and the weather model, the weather forecasting summary that being shared on social media is the prediction that made by the meteorologists. If the weather model is being expanded for detecting range of larger area and longer period, it is known as climate model.

Fundamentally, the climate model is similar with the weather model but there is extension in broader region and longer timespan. It helps in predicting the changing in average climate condition over years, decades or even more. The climate model will be focusing on the relationship among land, oceanic and atmospheric process to monitor the global warming. Although there are various types of climate models, they are basically generated from combination of mathematical equations that almost perfectly simulate weather changing in the climate system. With the help of climate model, the researchers and scientists are able to validate their hypothesis and make conclusion on historical study or future prediction since it gave a clearer picture to study the climate system. Besides, the researchers are able to find out the extraordinary weather event that induced by the climate change. It is very important to know the potential of an extreme event could happen for the disaster management, for example, the number of heavy rainfall event could happen during monsoon season in Malaysia.

Energy balance model, intermediate complexity model and general circulation models are three major category of models being widely utilized in meteorology field. The energy balance models take Earth's energy budget into account and helps to determine the climate change. The Earth's energy budget is referring to simulation of the heat exchange happen in natural environment. For example, resultant heat from solar energy, albedo and natural cooling effect on the earth due to reflection. The researchers try to combine the difference of the amount of input energy and output energy together and then generate an equation that shows the change in heat storage. Then, it will be combined with the models that representing the land in three-dimensional grid and used to simulate the local climate for a region. Next, the intermediate complexity model is similar with the previous models but it takes geographical structures such as land, ocean and glaciers into consideration. It is suitable for climate scenarios that only little changes over a long time, such as glaciers movement, oceanic flow changes or variation of chemical composition in the air. Third, the general circulation model (GCM) is suitable for my research since it consists of adequate and precise variables to simulate the potential climate change. General circulation model is capable of simulating the potential global climate change due to elevated greenhouse gas emission by representing the physical atmospheric and oceanic processes (Saha, Zeleke and Hafeez, 2019). It is a three-dimensional grid model with relatively finer resolution when comparing to the others. Indeed, it is more practical than the two models but it is time consuming for its outcome.

The historical station data helps in improving the accuracy of model to simulate the real climate system as a reference for future event. A reliable model could monitor the variation of climate system and helps in proposing any climate hazard mitigation to protect the environment. Normally, the accuracy of a model is determined based on the comparison of outcome with the historical data. The model is good as long as the difference between outcome and the historical data is zero which also indicates that good at predicting future event. Nevertheless, model always come with uncertainty no matter how good it is, and high resolution for small area region will give more reliable results. That is the reason why the climate models are needed to be in high resolution most of the time. The melting glaciers, rising of sea level and coastal erosion as the result of climate change, and the climate model gave us a precise understanding towards the influence of both natural and human activities to the climate system. The prediction can visualize the scenario that how is the climate pattern could behave if there are no change human activities and suggest the related agencies how to mitigate the anthropogenic climate change.

2.2.1 The General Circulation Models

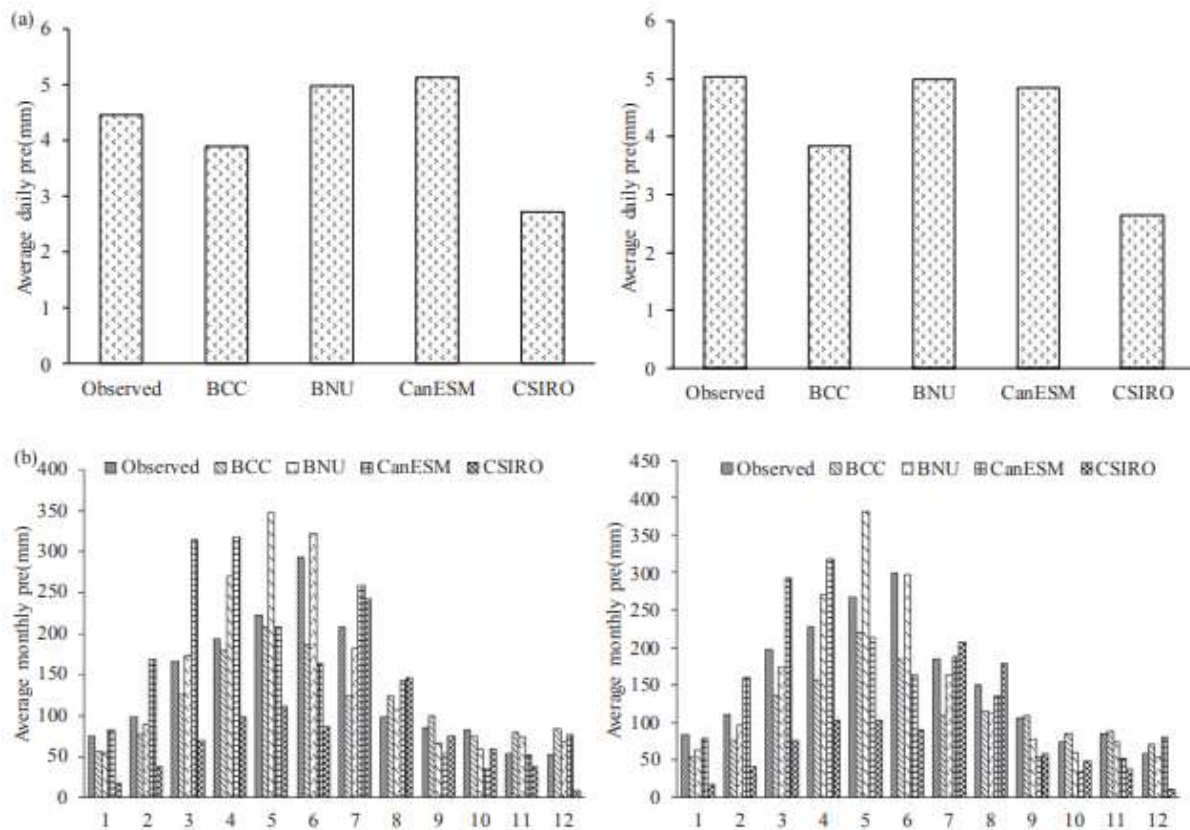
The Representative Concentration Pathway (RCP) is greenhouse gases concentration, instead of gas emission, scenario that approved by the Intergovernmental Panel on Climate Change (IPCC). The level of RCP is evaluated depends on the radiative forcing which is referring to the difference between incoming solar irradiance and radiated solar irradiance from Earth. Based on Table 3, the RCPs are divided into 4 levels with an effective duration until 2100. For expectations of the concentration pathway after 2100 are defined as Extended Concentration Pathways (ECP). In order to produce a good future climate estimation, suitable model should be considered for various criteria. In Xuan et al (2017), there were 18 models in the Coupled Model Intercomparison Project Phase 5 (CMIP5) being evaluated and 4 out of them were chosen that has better future climate estimation under RCP4.5 and RCP8.5 in their study. Based on monthly and seasonal variables, the results of performance comparisons under 3 evaluation indices, correlation coefficient (R), root mean square error (RMSE) and model estimation bias percentage (PBIAS), are stated in Table 4. According to the outcome, BCC-CSM 1-1 and BNU-ESM are the main choices, and then CanESM2 and CSIRO-Mk 3-6-0 come after with reasonable good performance. In Gao et al (2020) research, the four models, BCC, BNU, CanESM and CSIRO, were used for future peak flow and flood level forecasting. To determine the performance of each models, 5 evaluation indices in average for multi-years, simulated precipitation, monthly precipitation, seasonal precipitation, annual maximum 1-day precipitation and annual maximum precipitation in 5 days consecutively, were considered. The last two maximum cases indicate extreme scenario while the first three indicates the mean scenarios. Based on Figure 4, each models, in short, have their own pros and cons in terms of performances. The underestimated simulation of measured precipitation always happen in the BCC model. The simulations of CSIRO are always underestimating the measured mean values but it simulated good results in extreme values. Both BNU and CanESM are capable of simulating good results as a whole but there are serious fluctuations in monthly average precipitation in few months.

Table 3 Classification of RCPs.

Representative Concentration Pathway	Definitions & ECP assumption
RCP 2.6	-The peak of this pathway is approximately 3 W/m ² then decline to 2.6 before 2100. -concentration remain constant after 2100.
RCP 4.5	-The pathway will stabilize at 4.5W/m ² approximately after 2100. -concentration remain constant after 2150.
RCP 6.0	-The pathway will stabilize at 6.0W/m ² approximately after 2100. -concentration remain constant after 2150.
RCP 8.5	-The pathway is approximately greater than 8.5 W/m ² by 2100 and keep rising for a period. -Constant emission after 2100 & constant concentration after 2250.

Table 4 The performance of models under 6 variables (Xuan et al., 2017).

Climatic variables	Order of GCMs
Maximum temperature (monthly $R>0.90$, RMSE<3, absolute BIAS<1 °C)	BNU-ESM, CanESM2, MIROC5, MIROC-ESM, MIROC-ESM-CHEM, MPI-ESM-LR
Minimum temperature (monthly $R>0.90$, RMSE<3, absolute BIAS<1 °C)	BNU-ESM, CNRM-CM5, CSIRO-Mk3-6-0, GFDL-ESM2G, GFDL-ESM2M, HadGEM2-ES
Precipitation (seasonal $R>0.80$, RMSE<100, PBIAS<15 %)	BCC-CSM1-1, BNU-ESM, CanESM2, CSIRO-Mk3-6-0, GFDL-CM3, GISS-E2-H, GISS-E2-R, IPSL-CM5A-LR, MPI-ESM-LR, MRI-CGCM3
Wind speed (seasonal $R>0.80$, RMSE<2, PBIAS<20 %)	BCC-CSM1-1, BNU-ESM, CanESM2, CSIRO-Mk3-6-0
Solar radiation (monthly $R>0.80$, RMSE<40, PBIAS<10 %)	BCC-CSM1-1, BNU-ESM, CanESM2, CSIRO-Mk3-6-0, GFDL-ESM2G, GISS-E2-H, GISS-E2-R, HadGEM2-AO, HadGEM2-ES, MPI-ESM-LR
Relative humidity (seasonal $R>0.80$, RMSE<15, PBIAS<10 %)	BCC-CSM1-1, BNU-ESM, CanESM2, CNRM-CM5, MI-ESM-LR



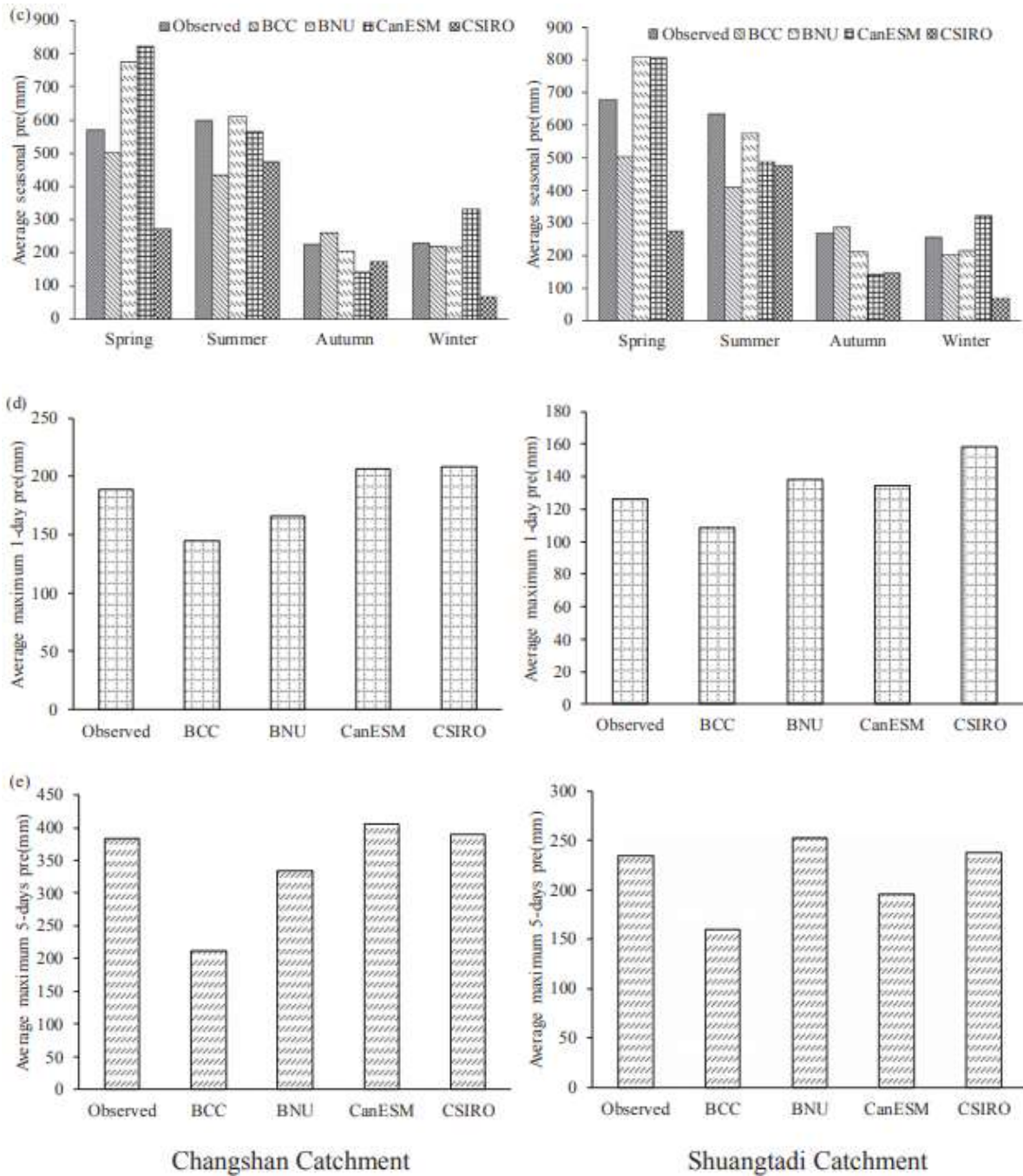


Figure 4 Performances of 4 models under a) multi-years average simulated precipitation. b) multi-years average monthly precipitation. c) multi-years average seasonal precipitation. d) multi-years average annual maximum 1-day precipitation. e) multi-years average annual maximum precipitation in 5-days consecutively (Gao et al., 2020).

2.3 Regional Climate Model

Although there are various climate models can simulate the atmospheric conditions, yet each model simulates the atmospheric variation at different scales over the Earth surface. The General Circulation Models (GCMs) in low resolution are being widely utilized for the development of climate change scenario or for the fundamental studies. Most of the time, the

models will be downscaled into a higher resolution model to obtain local climate variables because they cannot be utilized for regional climate study at such low resolution (Roux *et al.*, 2017). The downscaling of a model is to bridge the gap between large-scale and local-scale climate variables and it is being categorized into two fundamental approaches, dynamical downscaling and statistical downscaling. In this research, the statistical downscaling will be chosen due to resources restriction. For a better understanding to differentiate both approaches, there are some characteristic of both approaches shown in Table 5. For this research, the statistical downscaling approach is chosen as its outcome resolution is sufficient for the study and it takes shorter time to get the outcome.

2.3.1 Dynamical downscaling

It is a model that simulating local climate responses by nesting the Regional Climate Model into the GCM. It resolves the regional climatic process in a consistent way physically and simulates the variables in medium-scale. It is an approach that capable of simulating the dynamic regional climate system. According to Roux *et al* (2017), the dynamical downscaling method to get the variables in higher resolution is very tedious and time consuming. Besides, the dynamical downscaling approach is subject to the availability of intensive computational resources such as super computer, so there is a limitation on number of GCMs available (Shamir *et al.*, 2019).

2.3.2 Statistical downscaling

Statistical downscaling approach comes with an assumption that the statistical relationship between the predictors (GCM) and predictand (observed station data) remain constant over the time therefore they are stationary (Carpenter and Georgakakos, 2001). As comparing to dynamical downscaling approach, statistical downscaling approach is relatively user-friendly without much rely on the intensive computational resources. Plus, it could be applied for generating high resolution variables and large number of GCMs input.

Table 5 Characteristic of dynamical and statistical downscaling approaches (Roux et al., 2017; Kotamarthi et al., 2016; Gutmann et al., 2012; Sunyer et al., 2012; Boe et al., 2007).

Dynamical downscaling	Able to simulate dynamic (continuously) regional climate model. Iterations for high resolution variables are tedious and time consuming. Requirement on intensive computation resources.
Statistical downscaling	Only downscaling one climatic variable at one time. Climatic variables remain constant over the time. Lesser requirement on intensive computation resources. Produce acceptable results with shorter duration. Better outcome for temperature and precipitation when running a hydrological model. Poor at representing the changes in spatial pattern of winter precipitation over complex terrain.

2.4 Climate hazard

Needless to say, the growth of global population and elevation in demand are major drivers that expand the influence of climate change globally. As a result of global warming, the occurrence of extreme climate event become more frequent and intensive. Climate hazard is referring to a physical climatic responses or event which relating to hydro-meteorological or oceanographic phenomena that has the potential to damage property, health or natural resources (Brooks, 2003). Basically, drought and flood are the two potential climate hazard could happen in Malaysia (Latif and Mustafa, 2020; Tan *et al.*, 2020; Soh *et al.*, 2018; Huang *et al.*, 2016). Flood is always spotted after a downpour and it is becoming the significant hydrological issue in Malaysia. Due to the climate change, the design of current drainage system is not capable of handling the rainfall amount. According to Latif and Mustafa (2020), lack of complete hydrograph is one of the factors that cause failure of flood defence in Malaysia. Besides that, the drought is severe issue that can impact both economy and agriculture sectors because plantation is one of the major livelihoods to Malaysians and the agriculture products, such as palm oil and rubber, is one of the Gross Domestic Production (GDP) major contributors (Alam *et al.*, 2020). Plus, the total population of Southeast Asia is 662 million in 2019, approximately equals to 8.5% of global population (UN, 2019), and the pressure on environment grow with population. In the other words, the water and food supply could be critical since drought could bring dryness issues such as damage on crops, forest fire and reduction on water resources (Tan *et al.*, 2014). In the end, the climate hazards impact the country development and the economy growth adversely.

2.5 Past studies

In the meteorology study, the global circulation models are being developed to simulate the real world climatic changes in the past or future in order to determine the consequences earlier. The outcome of the model is valuable data to disaster management since it can help in preparing for necessary adaptation measures by the forecasting trend. Basically, these climate model is in a coarse resolution to ease the study at large scale. Due to the low resolution of the raw data of GCMs, the downscaling approach is a compulsory procedure in climate modeling. In order to test the reliability of the model, the variation of the model will be carried out by comparing the historical data and the simulated data for a baseline period. Based on Feyissa *et al.* (2018) study, both maximum and minimum temperature and precipitation in Addis Ababa for 30-year durations are being downscaled statistically to determine the future responses and extremes. The climatic variables are taken from the second generation of the Earth System Model (CanESM2) and Coupled Global Climate Model (CGCM3) under Representative Concentration Pathways (RCP) Scenarios, RCP4.5 and RCP8.5, and Special Report Emission Scenarios (SRES), A1B and A2. Due to consideration for completeness of data and good location representation, two meteorological stations were chosen at different elevation. Addis Ababa station with altitude 2386 m represents the urban center region when Entoto station with altitude 2903 m represents suburban region. When selecting the predictors, the correlation statistics and p_value are the main criteria for selection and the SDSM is capable of managing the task of screening variables. In modeling, the higher the correlation values, the stronger relationship and the smaller the p-value, the stronger the evidence to prove that there is relationship between two variables (Brereton, 2019). The calibration and validation period for

two station is shown in the Table 6. During model calibration, the coefficient of determination (R^2) and Standard Error (SE) factor are considered. After calibration of model, the data provided by National Central of Environmental Prediction (NCEP) was used for comparison of model output in validation stage and the results are shown in Table 7. In Table 8, the downscaled model predicted that the highest difference of precipitation is 16.6% and 8% at Addis Ababa and Entoto station respectively in 2080s under RCP8.5 and CanESM 2. Due to high urban activity and climate change, it was concluded that the city would experience an elevation in temperature. Plus, the potential of flooding event is expected high due to rising of precipitation. It consists of proper model calibration with strong correlation predictors and validation with reliable historical data.

Table 6 Test duration of modeling for Addis Ababa and Entoto stations (Feyissa et al., 2018).

Station	Calibration period	Validation period
Addis Ababa	1971-1985	1986-2000
Entoto	1989-1998	1999-2003

Table 7 The result of model calibration and validation (Feyissa et al., 2018).

Model	Addis Ababa obs. Calibration Period (1971–1985)			Addis Ababa obs. Validation Period (1986–2000)		
	Maximum Temperature	Minimum Temp	Precipitation	Maximum Temperature	Minimum Temp	Precipitation
	R^2	R^2	R^2	R^2	R^2	R^2
	SE	SE	SE	SE	SE	SE
NCEP	0.63	0.68	0.09	0.58	0.63	0.02
	1.34	1.21	9.02	1.45	1.12	9.55
CanESM2	0.63	0.66	0.011	0.57	0.65	0.01
	1.36	1.18	9.00	1.46	1.17	9.50
CGCM3	0.64	0.66	0.01	0.58	0.64	0.06
	1.34	1.17	9.00	1.44	1.17	9.58
	Entoto Station Calibration Period (1989–1998)			Entoto Station Validation Period (1999–2003)		
NCEP	0.58	0.65	0.031	0.60	0.40	0.01
	1.32	1.10	9.30	1.4	1.00	8.20
CanESM2	0.62	0.64	0.043	0.63	0.41	0.04
	1.35	0.09	9.30	1.36	0.97	8.20
CGCM3	0.61	0.65	0.030	0.62	0.43	0.04
	1.36	1.10	9.37	1.38	1.00	8.22

R^2 : Coefficient of determination; SE: Standard Error. Autoregressive terms are added on all R^2 and SE values in SDSM.

Table 8 Temperature and precipitation with various scenarios from downscaled modelling (Feyissa et al., 2018).

Station	Predictands	Year	CanESM2		CGCM3	
			RCP4.5	RCP8.5	A1B	A2
Addis Ababa obs. (Baseline period 1971–2000)	Maximum Temperature	2020s	0.09	0.06	0.09	0.12
		2050s	0.41	0.61	0.77	1.00
		2080s	0.52	1.20	1.31	2.06
	Minimum Temperature	2020s	0.02	0.02	0.36	0.07
		2050s	0.239	0.39	0.18	0.14
		2080s	0.30	0.70	0.28	0.27
	Precipitation (% Difference)	2020s	1.28	1.30	1.08	2.30
		2050s	3.82	6.20	4.02	8.70
		2080s	7.49	16.6	7.40	11.7
Entoto (Baseline period 1989–2003)	Maximum Temperature	2020s	0.09	0.09	0.17	0.21
		2050s	0.22	0.41	0.57	0.56
		2080s	0.28	0.71	0.84	1.01
	Minimum Temperature	2020s	0.03	0.03	0.25	0.20
		2050s	0.07	0.09	0.69	0.57
		2080s	0.10	0.14	1.04	0.99
	Precipitation (% Difference)	2020s	1.10	0.60	1.24	1.36
		2050s	2.57	4.80	2.80	2.70
		2080s	2.58	8.00	7.80	11.8

Notwithstanding the flooding is the most concerned extreme event, drought monitoring and forecasting is important for disaster management as well (Bachmir et al., 2016). Drought forecasting study with artificial intelligence models by Soh et al. (2018). In the study, the future Standardized Precipitation Evapotranspiration Index (SPEI) with different time scale (1, 3 and 6-month intervals) at the Langat River Basin, Malaysia was being forecasted with two hybrid models, Wavelet-ARIMA-ANN (WAAN) model and Wavelet-Adaptive Neuro-Fuzzy Inference System (WANFIS) model. Essentially, the SPEI is the drought evolutionary stages which developed with the resultant response due to precipitation, temperature or evapotranspiration (Beguer á, 2014). After the screening of available data, three temperature and precipitation station each were chosen. The location and detail of chosen stations are shown in Figure 5 and Table 9 respectively. To improve the performance of the models, the input data of both models was pre-processed. The calibration period and validation period are 1976-2007 and 2008-2015 for both models respectively. It was found that the larger the time scale length, the higher the accuracy of the model outcome for both. According to the results from WAANN and WANFIS, the outcome of 1-month intervals consists of higher errors. Throughout the Figures 8-9, the researchers stated that the extreme outliers in SPEI-1 could not be found since it has high degree of fluctuating. Based on Figure 7 and 8, the WAANN is capable of producing results for 3-month and 6-month which are similar with the original data set. As concluded by the researchers, WANFIS gave the results at satisfactory level only for mid-term while WAANN has higher accuracy in both short and mid-term drought forecasting. Throughout the research papers, the WAANN model is feasible for drought forecasting since it provided higher accuracy of prediction in both short and mid-term drought events.



Figure 5 The location of meteorological stations in Langat River Basin, Malaysia (Soh et al., 2018).

Table 9 Details of the selected hydrometric stations at the Langat River Basin (Soh et al., 2018).

Station name	Station ID	Available data	Record's period
Pejabat JPS Sg. Manggis	2815001	Precipitation	1976–2015
P/K WLN P/S Telok Gong	2913001	Precipitation	1976–2015
RTM Kajang	2917001	Precipitation	1976–2015
Hospital Seremban	45241	Temperature	1976–2015
Ampangan Ulu Langat	44320	Temperature	1985–2015
Petaling Jaya	48648	Temperature	1976–2015

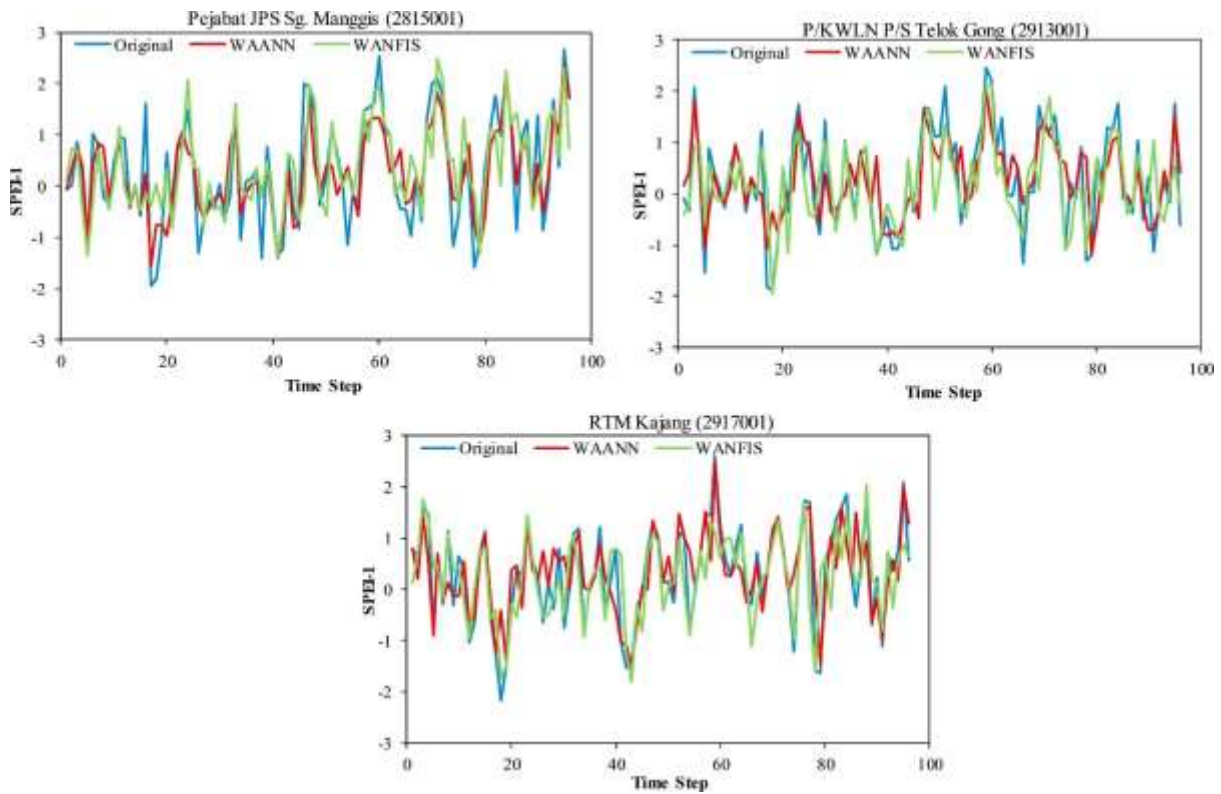


Figure 6 Plotting of SPEI with 1-month interval (Soh et al., 2018).

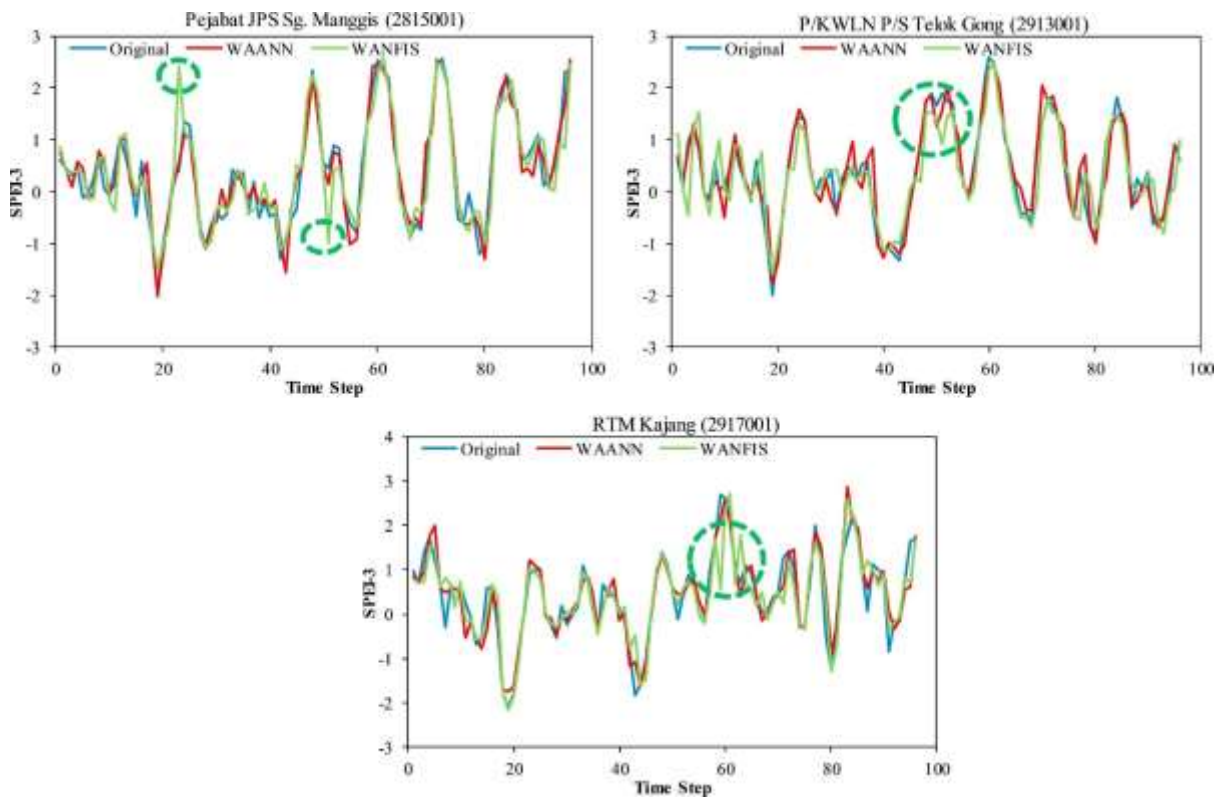


Figure 7 Plotting of SPEI with 3-month intervals (Soh et al., 2018).

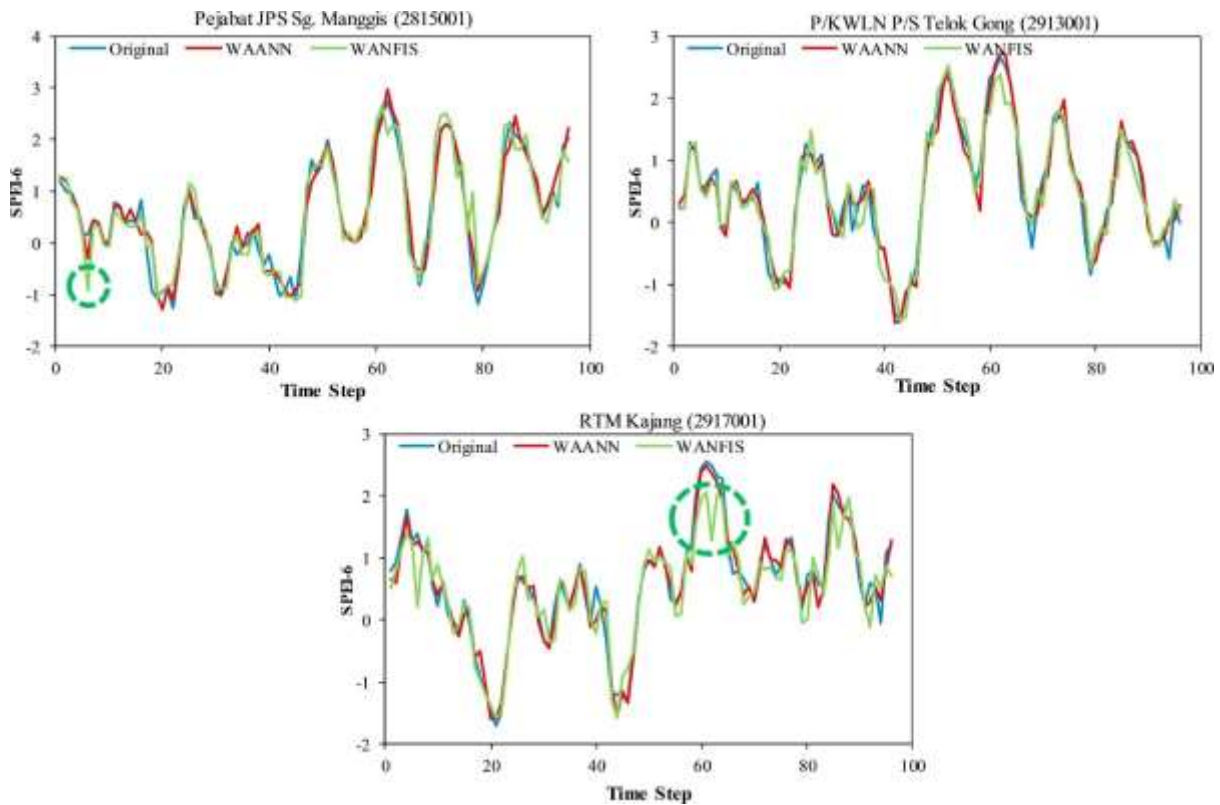


Figure 8 Plotting of SPEI with 6-month intervals (Soh et al., 2018).

According to Huang et al. (2016), drought is natural disasters that hardly to be detected and therefore drought monitoring by drought indices is very important for drought management. There is a comparison among the drought indices in various time intervals with a means in the study. Again, the Canadian Earth System Model (CanESM2) model was chosen for the input predictors to simulate the future rainfall in Langat River Basin under the Representative Concentration Pathway (RCP8.5) as the greenhouse gaseous emission will keep rising according is in the assumption. Besides, the National Central of Environmental Prediction (NCEP) Reanalysis data is input as predictor to develop statistical relationship with the station data. The computation of Standard Precipitation Index (SPI) were divided into observed SPI, 1976-2011, and futuristic SPI, 2016-2100. The computation for futuristic SPI is according to the observed SPI and the SPI value was generated by comparing with the mean and standard deviation between future and historical rainfall intensity. The SPI with time interval 1-month, 6-months and 12-months described the drought in meteorological, agriculture and hydrological respectively. The drought classification of SPI is shown in Table 10 in this research. Based on the Figure 16, the longest duration is 127 months starting from January 2016 by EDI computation. In terms of agricultural drought, the longest period of drought is expected to happen is 370 between 2016 to 2100 and the severe drought ($SPI < -1$) could only happen in two months of them. The summary of statistical data is shown in Table 11, the researchers also predicted that the future rainfall amount would increase since majority of average indices value are above 0. In my opinion, this research is good since the drought indices in this study is capable of monitoring the variation of a drought event.

Table 10 Drought classification (Huang et al. ,2016).

SPI	Drought classification
0.0~-0.99	Mild drought

-1.0~-1.49 Moderate drought
 -1.5~-1.99 Severe drought
 -2.00~ Extreme drought

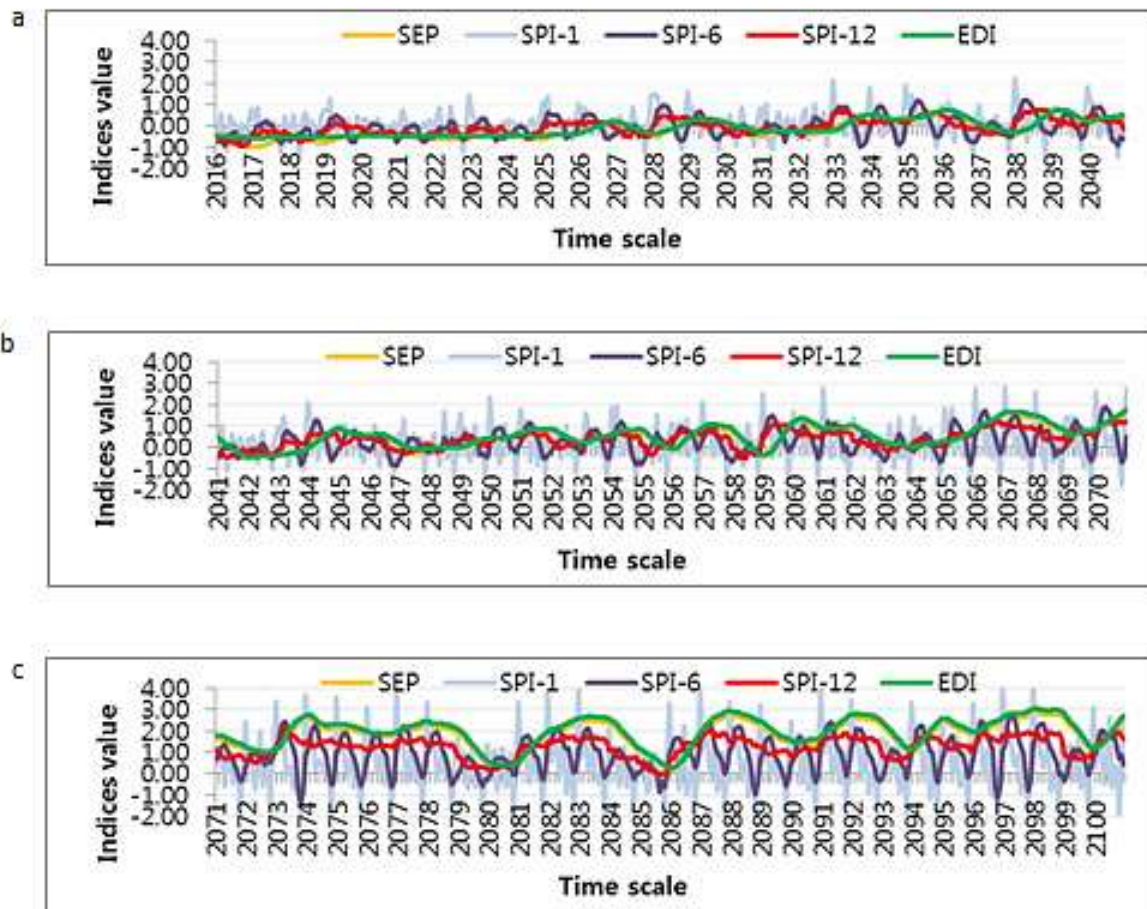


Figure 9 SEP, SPI-1, SPI-6, SPI-12 and EDI plotting for comparison a)2016-2040, b)2041-2070, c)2071-2100 (Huang et al. ,2016).

Table 11 Summary statistic of indices (Huang et al. ,2016).

Drought Index	SPI-1	SPI-6	SPI-12	SEP	EDI
Highest drought index	4.271	2.705	2.111	2.827	3.021
Lowest drought index	-0.914	-1.384	-0.908	-0.999	-0.560
Total amount of drought months (month)	363	370	245	271	259
Longest continuous drought months (month) and period	4 (Jul – Oct of year 2022, -23, -30, -33, -34, -36, -42, -46, -73, -74, -76, -88, -96, -97 & -98)	17 (Aug 17 – Dec 18 & Jul 23 – Nov 24)	67 (Jul 19 – Jan 25)	120 (Jan 16 – Nov 25)	127 (Jan 16 – June 26)

Based on Hussain *et al* (2017), the influence of climate change on the precipitation, maximum temperature and minimum temperature until 2100 in Sarawak state, Malaysia. The climate model is being proposed under the RCPs with the CanESM2 and the climate variables are downscaled by using the SDSM. The three meteorological stations involved are Kuching, Bintulu and Limbang. Overall, the temperature, under all selected RCPs, was estimated to elevate at the study area in Sarawak. Based on the simulation in Figure 10, the annual precipitation trend of Kuching and Bintulu are remaining unchanged but there will be lesser

precipitation in DJF and more in JJA due to seasonal shift. For Limbang station, the precipitation in future was estimated that more than historical precipitation. The researchers also suggested that make use of ensemble models to minimize the uncertainty due to single model estimation which is useful for further study.

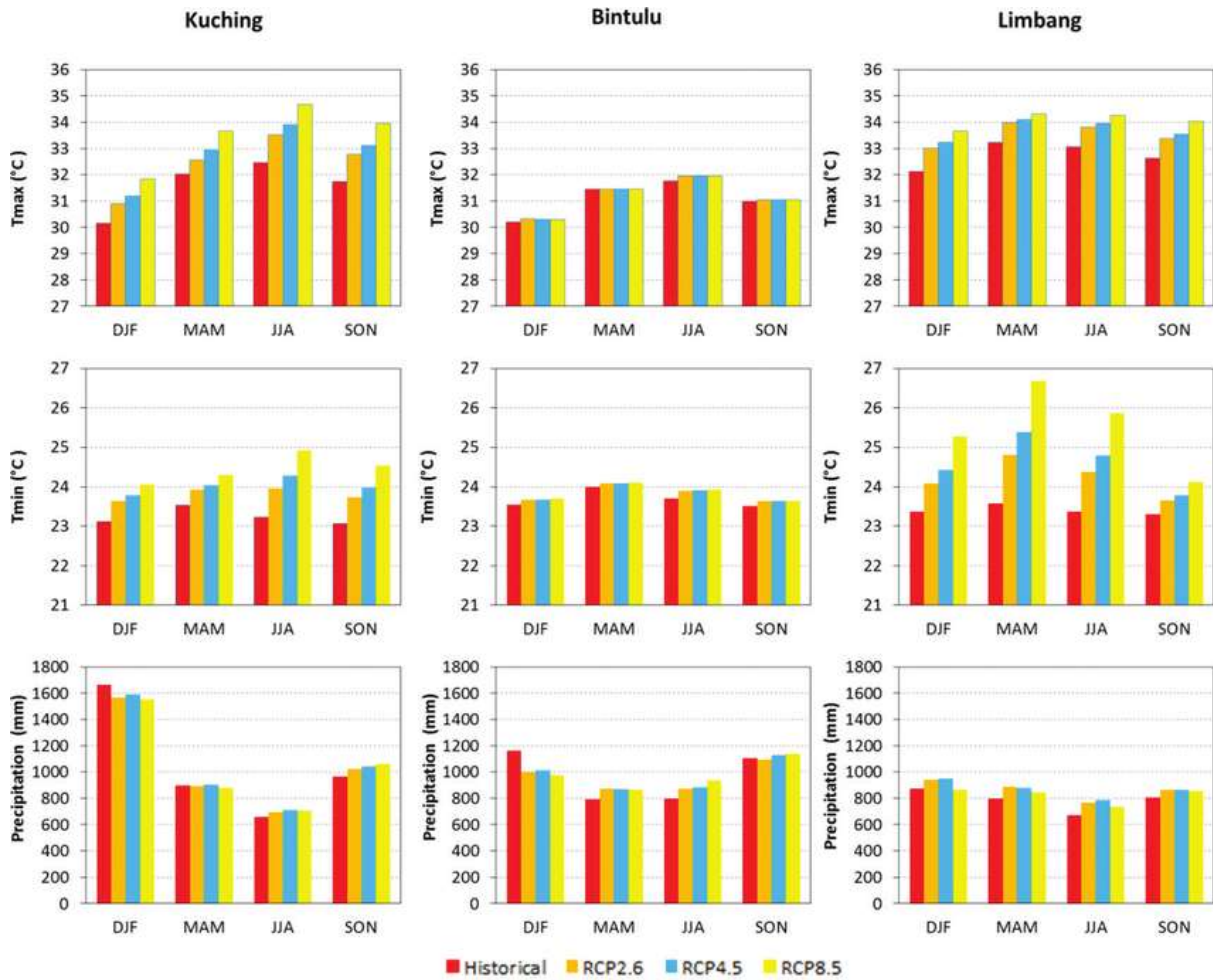


Figure 10 Seasonal changes for 2071-2100 at three stations (Hussain et al, 2017).

CHAPTER 3

METHODOLOGY

3.1 Workplan

In recent years, there are various meteorological studies related to CanESM2 as it can help in simulating the reliable local climate scenario. Initially, the precipitation and temperature in Kuala Krai, Kelantan was provided by the Malaysian Meteorological Department. The station is located at 102 °12' E, 05 °32' N with a height above mean sea level of 68.3 m and the available data was recorded from 1985 until 2019 as stated in Table 12.

Table 12 The selected station.

Station name	Station ID	Available data	Record's period
Kuala Krai	48616	Precipitation	1985–2019
		Temperature(mean)	1985–2013
		Temperature(max)	1985–2013
		Temperature(min)	1985–2013

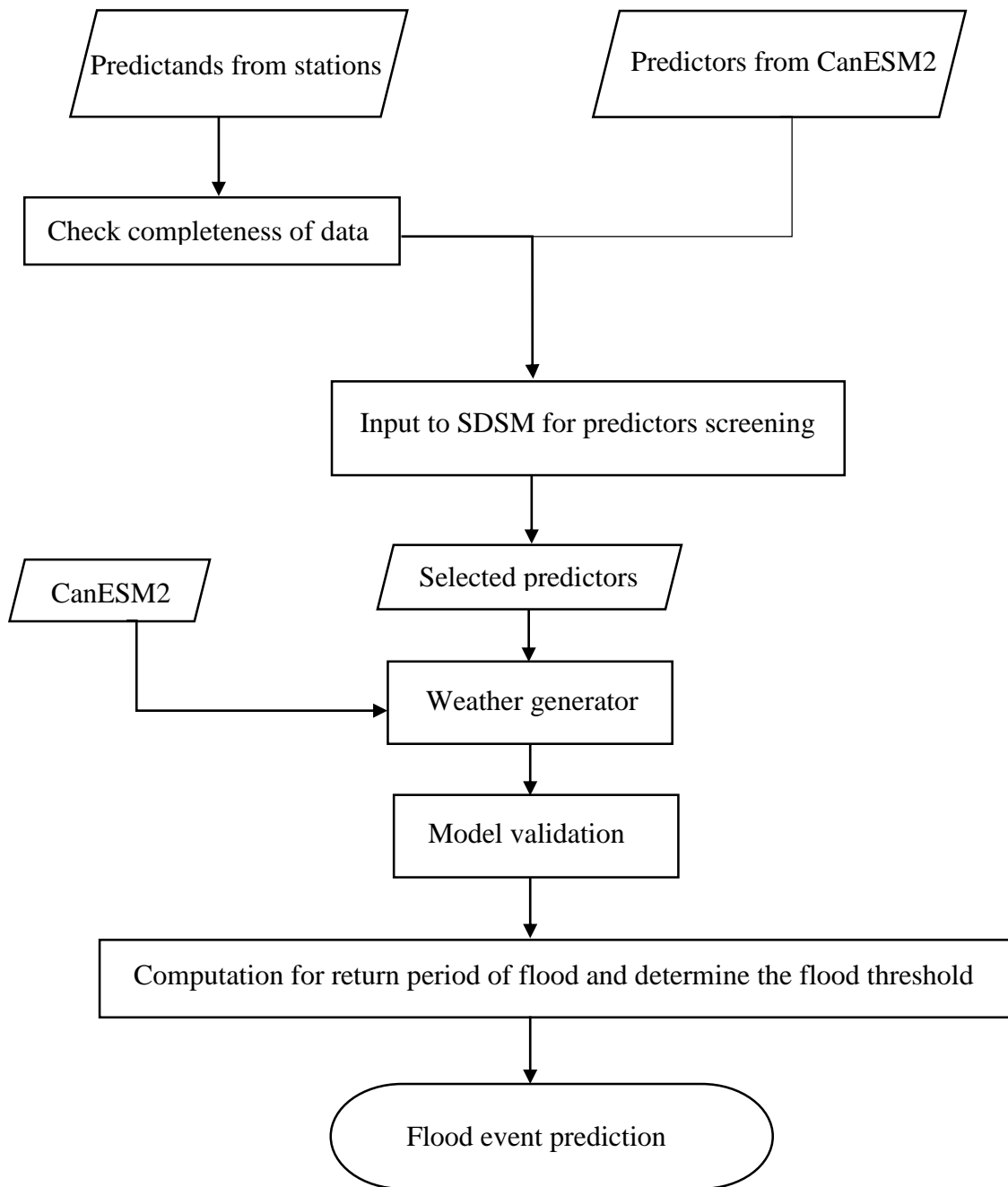
For predictors screening and calibration, these two phases are completed by using SDSM 4.2.9 (Figure 11) software.



Figure 11 SDSM software.

Then, model validation was conducted by linear regression, Pearson correlation and ANOVA test. If the model validation gives a satisfactory result which indicates that the model is reliable, the simulated data will be used for potential climate hazards assessment as following Figure 12.

Figure 12 Work flow chart.



3.2 CanESM2

The CanESM2 (Second generation Canadian Earth System Model) is the fourth generation model that developed by Canadian Centre for Climate Modelling and Analysis (CCCma) of Environment and Climate Change Canada. The goal of this project aims to propose the ensemble of daily predictors for the Coupled Model Intercomparison Project Phase 5 (CMIP5) and provide an approach that able to develop the predictors in a time and cost saving way. CanESM2 is one of the IPCC Fifth Assessment Report (AR5) contributors. The predictors provided by the CanESM2 are standardised historical daily values started recording from 1961 to 2005 and they are saved into a .dat files which is the file type can be import to the SDSM. The red dot plotted in Figure 13 is the location of station data (102 °12' E, 05 °32' N) at Kuala Krai.

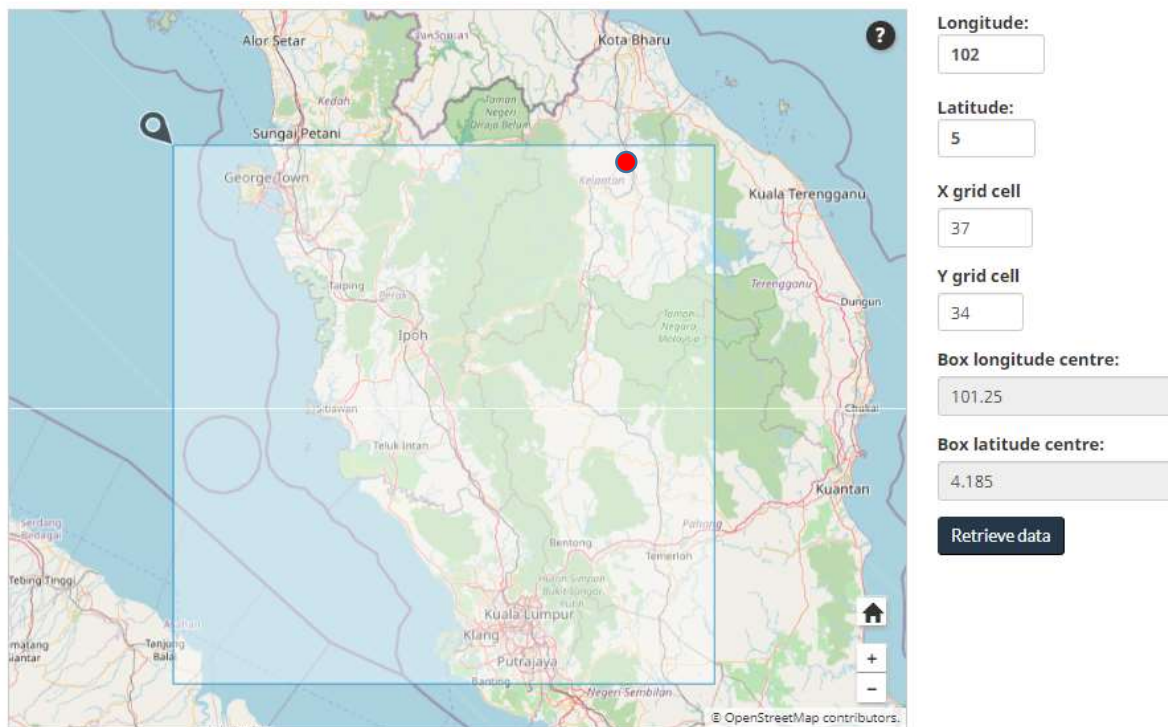


Figure 13 The CanESM2 predictors represents climate parameters for this cell covered region.

3.2.1 Predictors screening

In CanESM2, the earth domain is being divided into 128x64 grid cells, longitude-latitude direction, equally in total and the resolution of each cell is approximately 2.8125 ° along both the longitude and latitude uniformly. At the initial stage of modelling, the study region will be selected and there are total 26 predictors for that particular region will be extracted into a zip file. The descriptions of each predictor are shown in Table 13.

Table 13 The 26 predictors from CanESM2.

No	File name	Variable names
1	P*mslpgl.dat	Mean sea level pressure
2	P*p1_fgl.dat	1000 hPa Wind speed
3	P*p1_ugl.dat	1000 hPa Zonal wind component

4	P*p1_vgl.dat	1000 hPa Meridional wind component
5	P*p1_zgl.dat	1000 hPa Relative vorticity of true wind
6	P*p1thgl.dat	1000 hPa Wind direction
7	P*p1zhgl.dat	1000 hPa Divergence of true wind
8	P*p500gl.dat	500 hPa Geopotential
9	P*p5_fgl.dat	500 hPa Wind speed
10	P*p5_ugl.dat	500 hPa Zonal wind component
11	P*p5_vgl.dat	500 hPa Meridional wind component
12	P*p5_zgl.dat	500 hPa Relative vorticity of true wind
13	P*p5thgl.dat	500 hPa Wind direction
14	P*p5zhgl.dat	500 hPa Divergence of true wind
15	P*p850gl.dat	850 hPa Geopotential
16	P*p8_fgl.dat	850 hPa Wind speed
17	P*p8_ugl.dat	850 hPa Zonal wind component
18	P*p8_vgl.dat	850 hPa Meridional wind component
19	P*p8_zgl.dat	850 hPa Relative vorticity of true wind
20	P*p8thgl.dat	850 hPa Wind direction
21	P*p8zhgl.dat	850 hPa Divergence of true wind
22	P*prcpgl.dat	Total precipitation
23	P*s500gl.dat	500 hPa Specific humidity
24	P*s850gl.dat	850 hPa Specific humidity
25	P*shumgl.dat	1000 hPa Specific humidity
26	P*tempgl.dat	Air temperature at 2 m

The p_value is defined as the probability of obtaining a result would be equal to or more extreme than the observed value under no difference assumption (null hypothesis) (Brereton, 2019; Grabowski, 2016). In the other words, p_value is the evidence that reject the null hypothesis and a p_value indicates the probability of the null is correct. Therefore, a smaller p_value gives stronger evidence that the null hypothesis should be rejected and the results are statistically significant. In this research, significant level is 0.05 and predictors with $p_value \leq 0.05$ will be selected for model calibration.

When all the input data are screened by the SDSM, a file that consist of all the selected predictors were generated. During the screening process, the predictand (station data) and the 26 predictors were assessed by partial regression test, the correlation between predictand and the predictors were determined by comparing the trend pattern. Due to existence of strong relationships ($P \leq 0.05$), each of the selected predictors will have their own trends, may differ with others, which show correlation with the predictand. Nevertheless, based on repeating computation, the variables with p_value equals to 0 will give the most accurate result, so that it was selected as the selected predictors in Figure 14.

	Partial r	P value
ncepmslpgl.dat	-0.007	0.5076
ncepp1_fgl.dat	-0.008	0.4946
ncepp1_ugl.dat	0.011	0.4426
ncepp1_vgl.dat	-0.037	0.0393
ncepp1_zgl.dat	-0.020	0.2685
ncepp1thgl.dat	0.002	0.5609
ncepp1zhgl.dat	-0.073	0.0000
ncepp5_fgl.dat	-0.030	0.1014
ncepp5_ugl.dat	-0.034	0.0619
ncepp5_vgl.dat	-0.013	0.4105
ncepp5_zgl.dat	0.005	0.5375
ncepp500gl.dat	-0.030	0.0927
ncepp5thgl.dat	-0.032	0.0751
ncepp5zhgl.dat	-0.015	0.3608
ncepp8_fgl.dat	0.031	0.0875
ncepp8_ugl.dat	-0.017	0.3244
ncepp8_vgl.dat	-0.053	0.0022
ncepp8_zgl.dat	-0.005	0.5357
ncepp850gl.dat	-0.026	0.1461
ncepp8thgl.dat	-0.005	0.5339
ncepp8zhgl.dat	-0.037	0.0412
ncepprcpgl.dat	0.052	0.0026
nceps500gl.dat	0.040	0.0267
nceps850gl.dat	0.003	0.5568
ncepshumgl.dat	0.025	0.1666
nceptempgl.dat	-0.021	0.2304

Figure 14 Data screening for lag function -3.

3.2.2 Model calibration

The model was calibrated base on the baseline, 1985 to 2005 and simulation of daily rainfall for 2006 to 2018 were performed with the selected predictors. In order to minimize the uncertainty due to single model, the calibration steps were repeated for 20 times to produce ensembles model. After that, an average model was derived from them and the model is ready for validation, based on the Kuala Krai station data, from 2006 to 2018.

At weather generation phase, the RCP4.5 and RCP8.5 from the CanESM2 and the file generated from selected predictors were used in SDSM again to calibrate a climate model. Before calibrating the model, the type of process was chosen as conditional. Conditional model is used for climate parameter that depends on the occurrence of other parameters such as evaporation and precipitation while the unconditional is used for independent climate parameter such as temperature. Although there may have difference in trend of selected predictors, the outcome of the SDSM is the combination of all predictors become one trend. Ensemble models will be adopted to minimise the uncertainty due to single model (Hussain *et al*, 2017).

3.2.3 Model validation

The calibrated model was tested base on the validation period, 2006 to 2018. After that, ANOVA, linear regression and Pearson methods were applied for model validation by using Microsoft Excel. The selected predictors and RCP are the only factors that may result in the failure of validation. Therefore, if the validation is failed, the modelling would be repeated again, starting from the screening of predictors. It is a trial-and-error process, each time of trial of screening may result in different outcome. It is a time consuming process for more trial to get better screening outcome. Besides, the same group of screening predictors may have

different outcome under different RCP, this additional variable make process become challenging to determine the best outcome. If all the variations cannot generate a valid outcome, lag function method was introduced to increase the variability of the factors. The lag functions with 1,2,3,-1,-2 and -3 were used for further study.

3.2.4 Statistical analysis

The statistical analysis is an approach that able to determine the validation of the null hypothesis for decision making. Similar to the regression test, there are two hypotheses, null and alternative, will be stated out before the test, therefore there is at least one conclusion can be drawn due the rejection of the hypothesis. The null hypothesis is the assumption that one variable is manipulated by the another one while the alternative is referring to one variable is not manipulated by the another one. The different of these two test is that regression test determines the existence of relationship between two variables while the statistical test indicates the strength and direction of the relationship. In the biological field, the statistical test has been widely studied to determine the correlation of the traits (Zhao, Liu and Li, 2017; Marchini *et al.*, 2014; Royar-Carenzi and Didier, 2019). The input variable must be differentiated between parametric or non-parametric variable before testing. With the statistical input, the test will give a numerical outcome that acting as an evidence to prove if there is any correlation between two variables. For model reliability test, there are several choices for analysis to see how strong is the model to simulate the real environment correctly.

i. Analysis of Variance (ANOVA)

Analysis of variance (ANOVA) is a mechanism to prove the result of the experiment is significant or not (Vishwanatha *et al*, 2021). ANOVA is capable of determining if there is relationship exist between two groups or more than that by comparing them at the same time. The F_ratio, the ANOVA coefficient, able to determine the variability between groups and within groups. The null hypothesis of ANOVA is that there is no difference in all tested groups. If the F_ratio is close to 1, the null hypothesis is true that there is no difference between all tested groups, and the null hypothesis will not be rejected. The p_value in the analysis is referring to the probability of null hypothesis is true where it assumes everything is same. As the p_value is smaller than the significance level, the null hypothesis will be rejected.

$$F = \frac{MST}{MSE}$$

Where the F is ANOVA coefficient, MST is mean sum of squares due to treatment and MSE is the mean sum of squares due to error.

ii. Spearman's Rank-Order Correlation

This approach is mainly applied for nonparametric variables. The Spearman's correlation coefficient, ρ indicates the strength and direction of the relationship of ranked data (ranks). It can be ranged from -1 to +1 and the meaning of the value is concluded in Table 14. Therefore, as long as the ρ value is near to the 0, which indicates that there is correlation but it is insignificant.

Table 14 Description for ρ .

Spearman's correlation coefficient, ρ	Description
-1	Very strong negative relationship between ranks
0	No relationship between the ranks
+1	Very strong relationship between ranks

iii. Coefficient of Determination, r^2

This is an approach that make use of the square of the Pearson correlation coefficient, r_value to determine the strength and direction of the relationship between the variables (Edelmann *et al*, 2021). The proportion of r^2 indicates that the amount of response of the variation that can be explained by the model successfully. The coefficient of determination is always a positive value that in a range of 0 to 1. The closer the r^2 to 1, the stronger the model can explain the response in the variation.

iv. Linear regression

In software engineering, the regression test could be a software testing that use to verify the code variation if the system still functioning well or not after system update (Minhas et al, 2020). Essentially, there are two groups of variables, dependent and independent, will be the input of regression test. Generally, the regression test results in a numerical outcome that prove if there is relationship between them. The dependent can be manipulated by only one independent or even more than one.

v. Pearson correlation

Pearson correlation is used to measure the linear correlation between two variables (Erdeljić et at., 2011; Jebli et at., 2021). The correlation coefficient (r_value) indicates the linear relationship of the variables. If the relationship of two variables could be concluded by a least square line or regression line, $-1 \leq r_value \leq 1$, a straight line that describe the response of y -variable when there is changes in x -variable, it indicates that there is high correlation between the variables. For validation purpose, the Pearson correlation will be used to identify the most reliable model. For r_value , the higher the value is, the higher the degree of reliability. The negative in r_value indicates that the variable is also statistical significant yet it is inversely proportional with the variable description.

3.3 Computation for flood return periods

i. Downscaling process

Deterministic model will produce the similar outcomes without inherent randomness with a given initial data set (Robeva et al., 2013). Generally, the historical rainfall data is very important to the deterministic models and daily rainfall data was recorded in mm per day. Therefore, a downscaling of daily rainfall into hourly rainfall is necessary. Based on Ministry

of Environment and Water 2021, the minimum precipitation threshold within 4-hours duration was always used to predict the flash flood from happening. According to Rasel and Islam (2015), the hourly rainfall can be determined as long as 24-hours rainfall data is available. P_t is the desired hourly rainfall; P_{24} is the 24-hours rainfall data; t is the final rainfall duration.

$$P_t = P_{24} \sqrt[3]{\frac{t}{24}}$$

ii. Flood return period

In order to determine the return period, the annual peak daily rainfall intensities, in the Kelantan Flood Report, were recorded starting from year 2013 until 2017. Based on Önen and Bagatur (2017), there is simplified Gumbel's distribution method being applied for flood prediction. The rainfall intensities of each year were derived into 1-hour, 4-hours, 6-years, 8-hours, 12-hours and 24-hours. Then, the mean and standard deviation of various hours were determined. In order to compute the frequency factor, K_t , the unknown for Y_t , Y_n and S_n were determined first. Since the sample size is 30, so the reduced mean, Y_n and reduced standard deviation, S_n are 0.5362 and 1.1124 respectively based on Table 15. The Y_t was computed by the formula Equation 2 while the T is the return period of the flood. After obtaining frequency factor (K_t) from Equation 3, the flood event with T -year return period could be calculated through Equation 4. In the end, the rainfall intensity with unit of mm/hr could be determined by dividing the flood event with 1-hour, 4-hours, 6-years, 8-hours, 12-hours and 24-hours.

Table 15 The reduced mean and reduced standard deviation in Gumbel's extreme value distribution (source: https://uomustansiriyah.edu.iq/media/lectures/5/5_2019_04_22!08_22_05_PM.pdf).

TABLE -1 - REDUCED MEAN β_n IN GUMBEL'S EXTREME VALUE DISTRIBUTION										
N = sample size										
N	0	1	2	3	4	5	6	7	8	9
10	0.4952	0.4996	0.5035	0.5070	0.5100	0.5128	0.5157	0.5181	0.5202	0.5220
20	0.5236	0.5252	0.5268	0.5283	0.5296	0.5309	0.5320	0.5332	0.5343	0.5353
30	0.5362	0.5371	0.5380	0.5388	0.5396	0.5402	0.5410	0.5418	0.5424	0.5430
40	0.5436	0.5442	0.5448	0.5453	0.5458	0.5463	0.5468	0.5473	0.5477	0.5481
50	0.5485	0.5489	0.5493	0.5497	0.5501	0.5504	0.5508	0.5511	0.5515	0.5518
60	0.5521	0.5524	0.5527	0.5530	0.5533	0.5535	0.5538	0.5540	0.5543	0.5545
70	0.5548	0.5550	0.5552	0.5555	0.5557	0.5559	0.5561	0.5563	0.5565	0.5567
80	0.5569	0.5570	0.5572	0.5574	0.5576	0.5578	0.5580	0.5581	0.5583	0.5585
90	0.5586	0.5587	0.5589	0.5591	0.5592	0.5593	0.5595	0.5596	0.5598	0.5599
100	0.5600									

TABLE -2 - REDUCED STANDARD DEVIATION S_n IN GUMBEL'S EXTREME VALUE DISTRIBUTION										
N = sample size										
N	0	1	2	3	4	5	6	7	8	9
10	0.9496	0.9676	0.9833	0.9971	1.0095	1.0206	1.0316	1.0411	1.0493	1.0565
20	1.0628	1.0696	1.0754	1.0811	1.0864	1.0915	1.0961	1.1004	1.1047	1.1086
30	1.1124	1.1159	1.1193	1.1226	1.1255	1.1285	1.1313	1.1339	1.1363	1.1388
40	1.1413	1.1436	1.1458	1.1480	1.1499	1.1519	1.1538	1.1557	1.1574	1.1590
50	1.1607	1.1623	1.1638	1.1658	1.1667	1.1681	1.1696	1.1708	1.1721	1.1734
60	1.1747	1.1759	1.1770	1.1782	1.1793	1.1803	1.1814	1.1824	1.1834	1.1844
70	1.1854	1.1863	1.1873	1.1881	1.1890	1.1898	1.1906	1.1915	1.1923	1.1930
80	1.1938	1.1945	1.1953	1.1959	1.1967	1.1973	1.1980	1.1987	1.1994	1.2001
90	1.2007	1.2013	1.2020	1.2026	1.2032	1.2038	1.2044	1.2049	1.2055	1.2060
100	1.2065									

$$Yt = -\ln(\ln(\frac{T}{T-1})) \quad (Eq. 1)$$

$$Kt = \frac{(Yt - Yn)}{Sn} \quad (Eq. 3)$$

$$Xt = mean + STD * Kt \quad (Eq. 4)$$

3.4 Determination of flood hazard threshold

In order to determine the flood hazard threshold, the flood report which the historical flood events were recorded is the important data source. Based on Santos and Fragoso (2016), the flood threshold is defined as the minimum precipitation that could trigger the flood from happening. Consequently, the flood report was reviewed and the minimum precipitation that being recorded is the flood threshold in this case. At the same time, the peak precipitation in historical flood events were used to validate the flood hazard threshold as well. The review was starting from flood report in year 2012 until 2017, and the largest precipitation amount was noted. In the end, records represent five individual rainfall data for five years as shown in Table 16.

Table 16 Five individual rainfall data in the flood events.

Year	Intensity (mm/day)
2013	217
2014	129
2015	297
2016	245
2017	248

CHAPTER 4

DISCUSSION

4.1 Temperature (RCP4.5 & RCP8.5)

Initially, the model calibration involved different lag functions to determine a more reliable model. For Tmax calibration, lag function -3 was chosen and the predictors selected as shown below:

- ncepmslpgl.dat; $p = 0$; partial $r = -0.274$
- ncepp500gl.dat; $p = 0$; partial $r = 0.321$
- nceptempgl.data; $p = 0$; partial $r = 0.329$

For Tmin calibration, lag function -3 was chosen and the predictors selected as shown below:

- ncepmslpgl.dat; $p = 0$; partial $r = -0.424$
- ncepp500gl.dat; $p = 0$; partial $r = 0.377$
- ncepshumgl.dat; $p = 0$; partial $r = 0.341$
- nceptempgl.data; $p = 0$; partial $r = 0.283$

After calibrating the model for precipitation, maximum temperature (Tmax) and minimum temperature (Tmin), they were compared with observed model. Based on observation, the model, among lag function groups, with more similar trend as comparing to observed model was chosen. As a result, the model with lag function -3 was chosen, for precipitation, Tmax and Tmin as shown in Figure 15, 16 and 17 as they shown higher similarity.

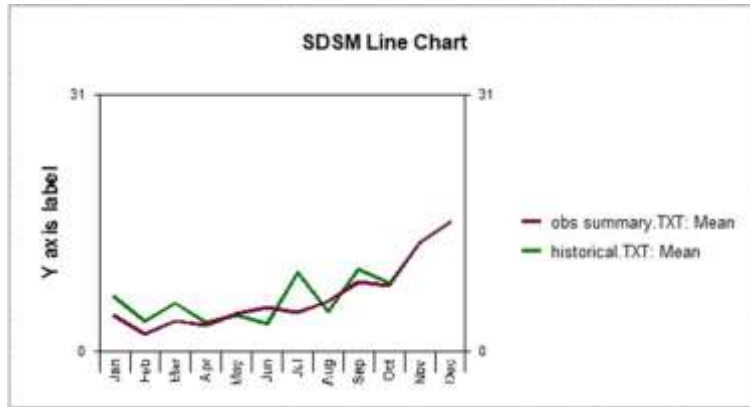


Figure 15 Precipitation model with lag function -3.

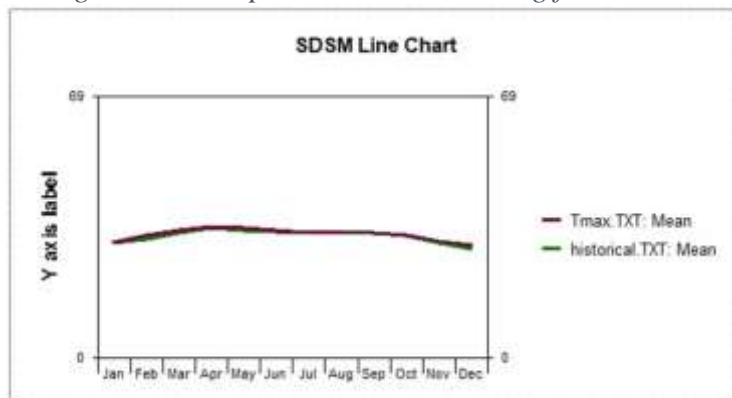


Figure 16 Tmax model with lag function -3.

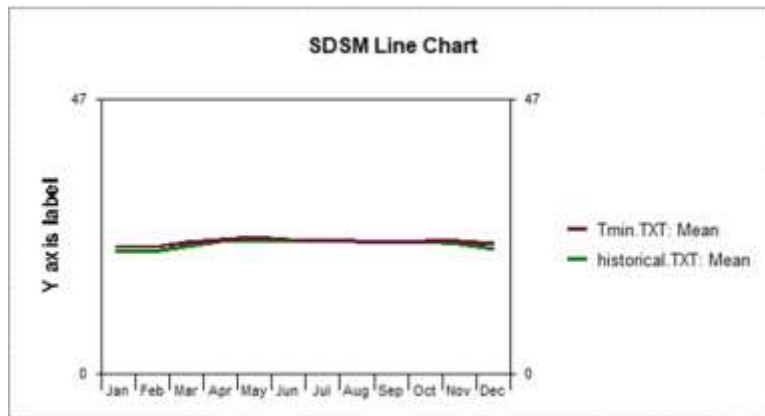


Figure 17 Tmin model with lag function -3.

According to the results of Probability Density Function (PDF) in Figure 18 and 19, the trend of simulated minimum and maximum temperature, 23°C and 32°C respectively, is having similar pattern as observed minimum and maximum temperature, 22.9°C and 32°C which is satisfactory. As a result, the future minimum and maximum temperature both were estimated to increase by 0.0154°C and 0.015°C per year respectively as shown in Figure 20. If the temperature increment last for 100 years, both minimum and maximum temperature is 1.5°C approximately above the current temperature. According to the Sixth Assessment Report (AR6)

produced by the Intergovernmental Panel on Climate Change (IPCC), when global warming reaching 1.5°C above pre-industrial level, the disaster and effect induced by the climate change will become irreversible. In the worst scenario, the Earth is projected to experience higher mean temperature, rising sea levels and intensive disaster. If this occur in Kuala Krai, the agricultural activities would be severely impacted due to adverse environmental changes such as saltwater intrusion.

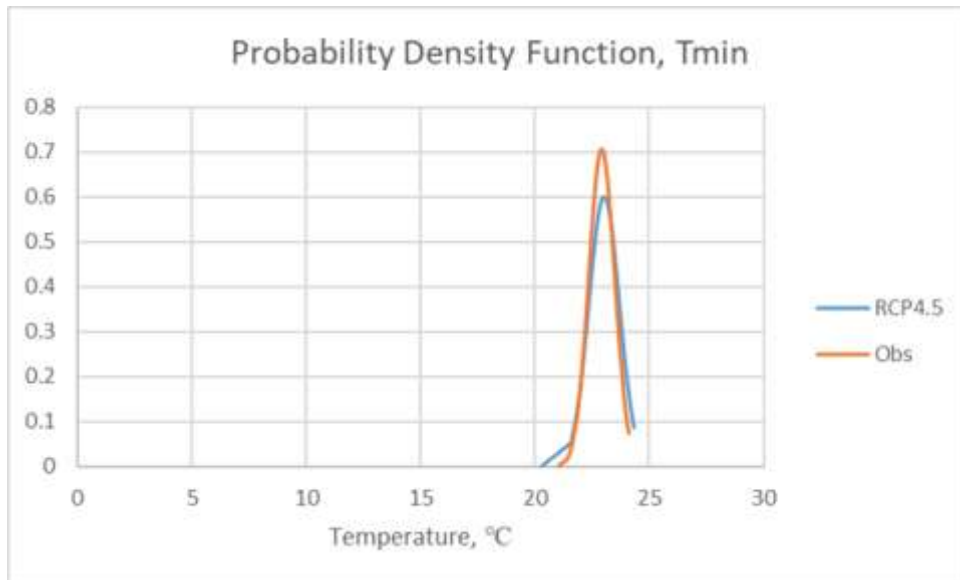


Figure 18 Probability Density Function of Tmin January 2006 to December 2013.

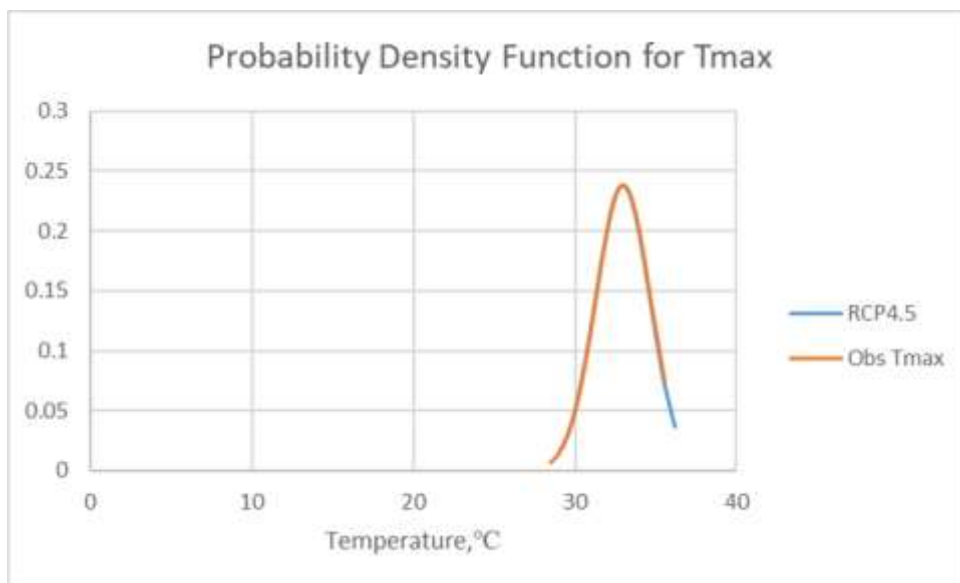


Figure 19 Probability Density Function of Tmax January 2006 to December 2013.

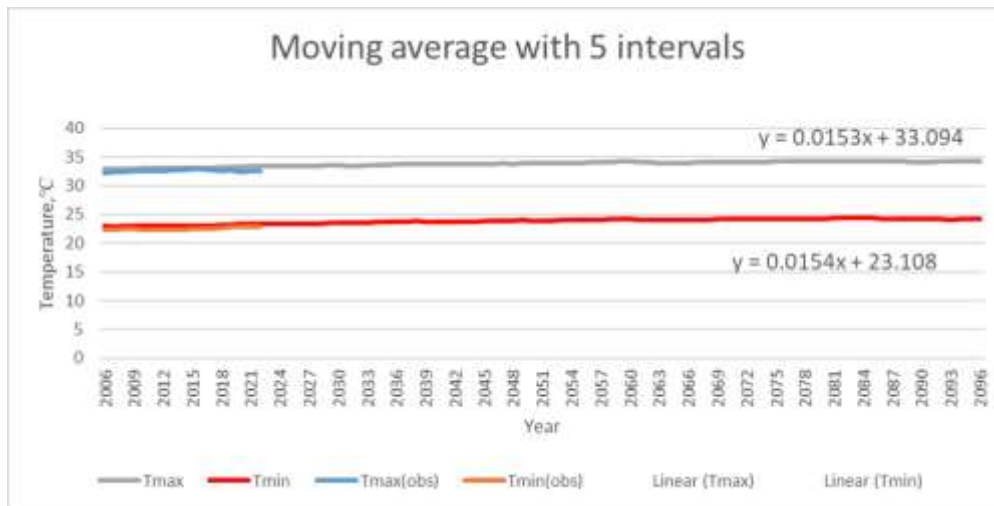


Figure 20 Estimation of future temperature.

4.2 Rainfall model (RCP4.5 & RCP8.5)

For rainfall model calibration under RCP4.5, the lag function -3 was chosen and the predictor selected as shown below:

- ncepp1zhgl.dat; $p = 0$; partial $r = -0.073$

According to rainfall model, the model can simulate the observed precipitation almost perfectly, but there were overestimation and underestimation in several months in Figure 15. Hence, the extreme cases were not simulated perfectly sometimes as shown in Figure 21. Based on (Tukimat et al., 2019; Gulacha and Mulungu, 2017), these errors are always found when comparing between observed and calibrated precipitation by using SDSM for modelling. Starting from January 2006 until May 2019, based on Figure 21, the mode of monthly precipitation is 210 mm for both observed and calibrated. Due to the common error of SDSM modelling, the extreme precipitation cannot be simulated by the model perfectly.

According to the reliability test result as shown in Table 17, the outcomes of ANOVA, Pearson correlation coefficient and linear regression test for RCP4.5 are 0.6726, 0.2290 and 0.5477 respectively; while RCP8.5 are 0.9845, 0.2813 and 0.5303 respectively. Based on Nahm (2017), the p_value in ANOVA test indicated that the probability of the simulated data is equivalent or even exceeding the actual data in the future. Therefore, smaller p_value will give more reliable results.

Pearson correlation coefficient and linear regression test are indicating that the relationship of simulated and observed data, and strong relationship will give larger value. As a result, the simulated future rainfall pattern under RCP4.5 is slightly reliable than RCP8.5. Nevertheless, there is absence of critical difference in the reliability test outcome of both cases, so the future precipitation is possible to be estimated by RCP8.5 as well. As a result, the future precipitation under RCP4.5 was expected to fluctuate between 3000 mm and 2500 mm in Figure 22.

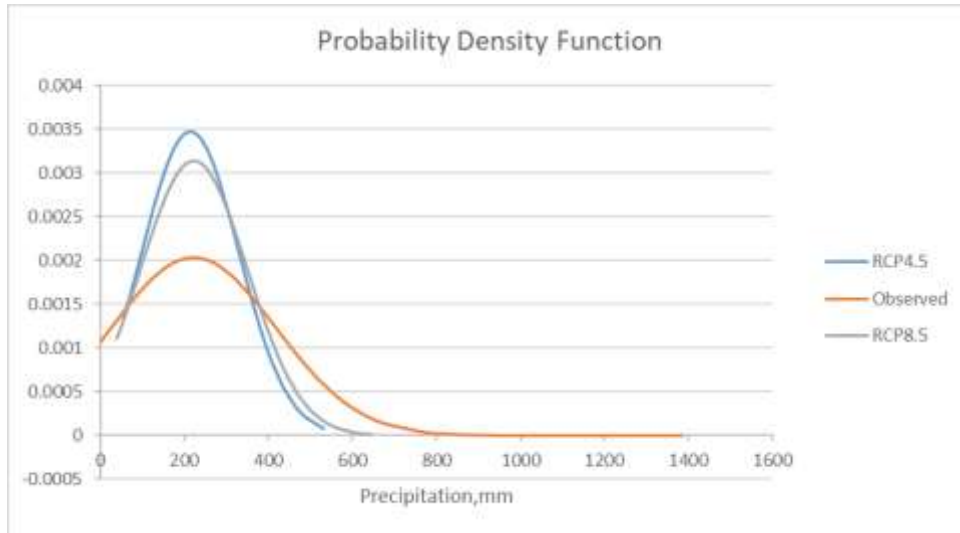


Figure 21 Probability Density Function of precipitation January 2006 to May 2019.

Table 17 Reliability test between RCP4.5 and RCP8.5.

Kuala Krai Station (Precipitation)		
	RCP4.5	RCP8.5
ANOVA (P-value)	0.6726	0.9845
Pearson Correlation Coefficients	0.2290	0.2813
Linear Regression	0.5477	0.5303

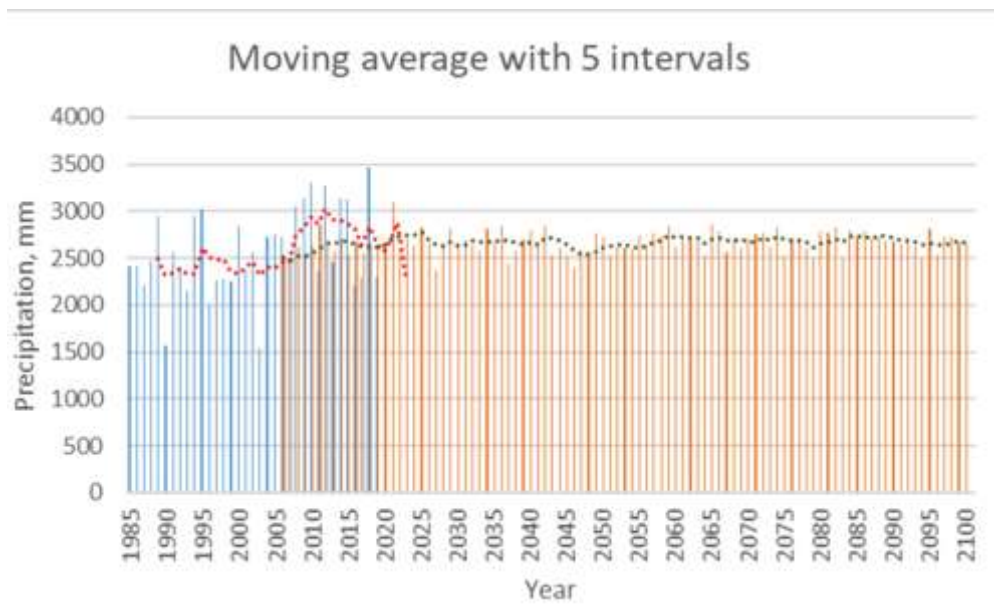


Figure 22 Estimation of future precipitation under RCP4.5.

4.3 Potential flood risk analysis

Normally, the rainfall will not induce flood easily as there is the maximum precipitation allowed before a flood will happen. Based on Santos and Fragoso (2016), flood threshold is referring to the minimum precipitation amount that could trigger the flood and cause overburden on drainage system. In Table 18, the flood reports indicate the rainfall data happened in Kuala Krai were analysed and downscaled into hourly rainfall. In Table 19, the minimum rainfall was determined in Kuala Krai, 2017 January 3rd and its threshold was 17.68 mm/hr. It is a flood threshold within 1-year interval. Based on Figure 23, the precipitation records of historical flood with various return periods are exceeding this threshold value which indicates this value is the critical level to trigger the flood. Hence, the 17.68 mm/hr was taken as the minimum threshold that may induce flood to the local region.

Table 18 Historical flood events happened in Kuala Krai.

Rainfall(mm/day)	Location	Date	Source
217	Kuala Krai	2013 Dec 3	Laporan_banjir_Kelantan_03122013_kemaskini_2
99	Kuala Koh	2013 Nov 30	Laporan_banjir_Kelantan_KualaKrai_03122013
129	Kuala Krai	2014 Dec 17	Laporan_banjir_Kelantan_20122014
87	Kuala Krai	2013 Jan 11	Laporan_banjir_Kelantan_11012013_kemaskini_1
103 (mm/hr)	Kuala Krai	2015 Dec 27	laporan_banjir_KualaKrai_27122015-1
100	Kuala Krai	2015 Dec 28	laporan_banjir_KualaKrai_28122015-2
183(mm/10hr)	Kuala Krai	2016 Dec 31	LBS 58 59 60 61 62 63 KELANTAN KUALA KRAI 31122016
32 (mm/6hr)	Kuala krai	2017 Jan 3	LBS 105 KELANTAN KUALA KRAI 03012017
141	Kuala Krai	2017 Jan 21	LBS_KELANTAN_KualaKrai_23012017
248	Dabong	2017 Jan 1	LBS81 KELANTAN TUMPAT 01012017
72	Kg Tualang	2017 Jan 24	LBS250 252 253_KELANTAN_KualaKrai_26012017

Table 19 Rainfall intensity of historical flood events.

mm/hr	mm/4hr	Location	Date
102.96	163.45	Kuala Krai	2015 Dec 27
85.98	136.48	Dabong	2017 Jan 1
84.94	134.83	Kuala Krai	2016 Dec 31
75.23	119.42	Kuala Krai	2013 Dec 3
48.88	77.60	Kuala Krai	2017 Jan 21
44.72	70.99	Kuala Krai	2014 Dec 17
34.67	55.03	Kuala Krai	2015 Dec 28
34.32	54.48	Kuala Koh	2013 Nov 30
30.16	47.88	Kuala Krai	2013 Jan 11
24.96	39.62	Kg Tualang	2017 Jan 24
17.68	28.07	Kuala Krai	2017 Jan 3

After obtaining the future daily rainfall from the model, the peak daily rainfall within a month is determined starting from year 2021 until the end of year 2100. After that, the peak daily rainfall data are derived into 4-hours and 1-hour rainfall intensity. Based on the results in Table

20 and 21, the precipitation that exceeding the flood threshold is 0.21% under RCP4.5 while probability of flood under RCP8.5 is 0.73%. According to both Table 20 and 21, the intensive precipitation can be found to happen in November and December more frequently. Malaysia is a tropical country that characterised by two monsoon season; monsoon in northeast part is starting from November until February and southwest region monsoon starting from May to August (Dhuha, et al., 2021). The potential of future flood event is low as comparing Figure 23 with Figure 24 and 25.

In the view of the comparison, the future precipitation estimation is lower than the historical flood return period and indicates that the future precipitation is almost under control. In the end, the heavy rainfall has higher potential to be observed in November, therefore the hydraulic structure as well as drainage repair project should be completed before November. In Kuala Krai, the logging activity at upstream is one of the factors causing flood. According to Samsurijan et al., (2018), the projects approved by Environmental Impact Assessment (EIA) were mainly located in Gua Musang, Kuala Krai and Tanah Merah since 2000 as shown in Table 22. Among those projects approved EIA, more than 80% of them were plantations, agriculture and forestry. It was found that the large-scale clearing in forest may increase the potential of flood in Kelantan even though the projects obtained EIA approval.

The logging activity could reduce the forest area directly, then the rain water become surface runoff directly since they could not be blocked by the natural barriers such as leaves and branches. When there is down pouring, precipitation creates a larger volume of surface runoff within a short period since there is no delay for water to contact with ground surface. The intensive surface runoff will erode the soil since the soil is not protected by the roots. As a result, the logging activity created an intensive surface runoff with the soil erosion that reducing the efficiency of the drainage system. Therefore, the Kelantan Forestry Department should amend the policy regarding the environmental impact with stringent policies on the logging activities.

Table 20 Peak daily rainfall under RCP4.5.

Month	Daily rainfall (mm/day)	4hr	2/960 days	1hr	2/960 days
Nov-95	51.673	28.43675	1	17.91403	1
Nov-23	51.57115	28.3807	1	17.87872	1
Nov-24	50.12875	27.58691	0	17.37867	0
Nov-78	48.678	26.78854	0	16.87572	0
Nov-67	46.8154	25.76351	0	16.22999	0
Nov-34	46.6012	25.64563	0	16.15573	0
Nov-91	46.3059	25.48312	0	16.05336	0
Dec-42	45.1539	24.84915	0	15.65398	0
Nov-88	44.58255	24.53472	0	15.45591	0
Nov-29	44.02025	24.22528	0	15.26097	0
Nov-62	43.94525	24.184	0	15.23497	0
Nov-40	43.5185	23.94915	0	15.08702	0
Nov-84	43.10105	23.71942	0	14.9423	0
Nov-52	42.8452	23.57862	0	14.8536	0
Nov-87	42.77565	23.54035	0	14.82949	0

Nov-80	40.4219	22.24503	0	14.01349	0
Nov-21	40.38625	22.22541	0	14.00113	0
Dec-85	40.2927	22.17393	0	13.9687	0
Nov-32	40.24475	22.14754	0	13.95208	0

Table 21 Peak daily rainfall under RCP8.5.

Month	daily rainfall (mm)	4hours	7/960 days	1hour	7/960 days
Nov-94	62.1492	34.20202	1	21.54592	1
Nov-44	61.84385	34.03398	1	21.44007	1
Nov-42	59.30225	32.63529	1	20.55894	1
Nov-87	59.25615	32.60992	1	20.54296	1
Nov-25	58.9762	32.45585	1	20.44591	1
Nov-68	56.08115	30.86265	1	19.44225	1
Nov-58	55.1535	30.35214	1	19.12065	1
Nov-96	50.45415	27.76599	0	17.49148	0
Nov-69	47.87785	26.3482	0	16.59832	0
Nov-98	47.41415	26.09301	0	16.43757	0
Nov-29	43.15415	23.74864	0	14.96071	0
Nov-30	43.15415	23.74864	0	14.96071	0
Nov-88	42.77005	23.53727	0	14.82755	0
Dec-40	42.5051	23.39146	0	14.7357	0
Nov-56	42.3461	23.30396	0	14.68057	0
Nov-71	41.8527	23.03243	0	14.50952	0
Dec-34	41.78325	22.99421	0	14.48544	0
Nov-82	41.6214	22.90514	0	14.42933	0
Nov-78	41.58675	22.88607	0	14.41732	0

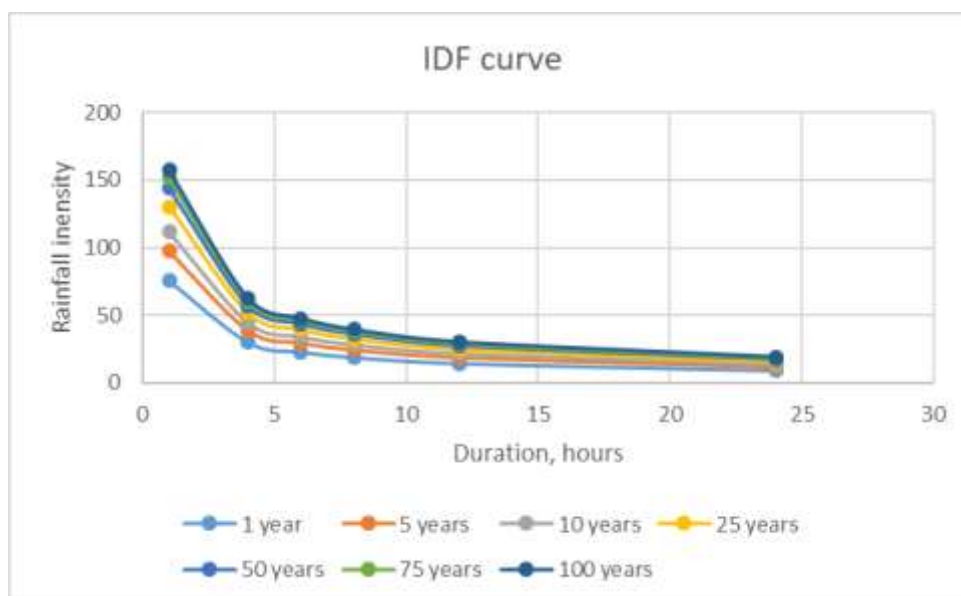


Figure 23 Return period of historical flood.

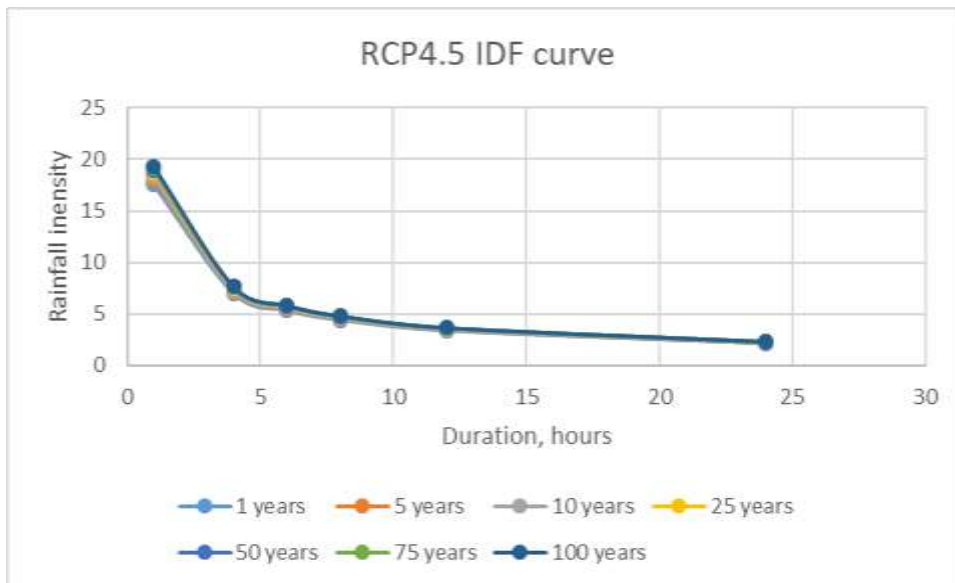


Figure 24 Return period under RCP4.5.

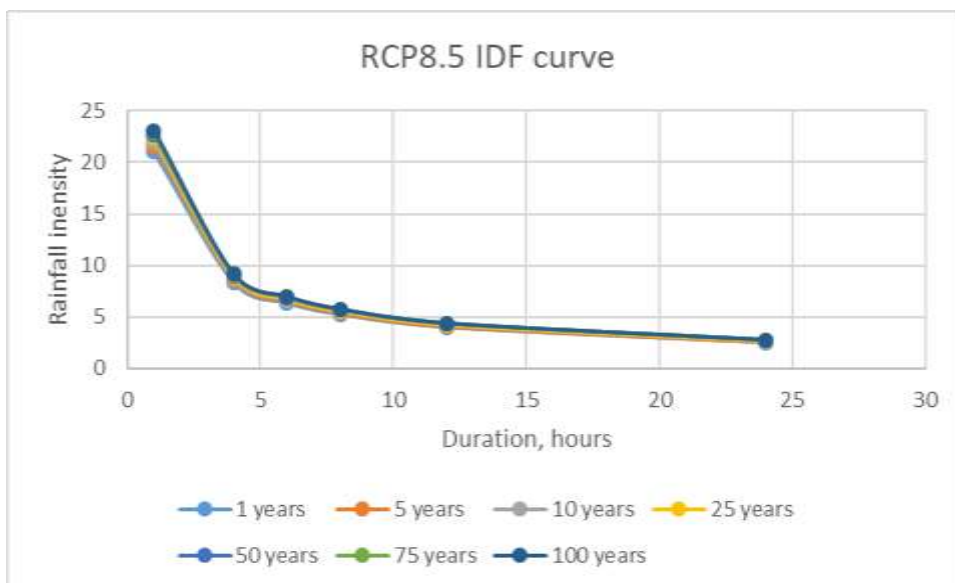


Figure 25 Return period under RCP8.5.

Table 22 Numbers of projects approved in Gua Musang, Kuala Krai and Tanah Merah (Samsurijan et al., 2018).

Year	Number of Projects Approved EIA		
	Gua Musang	Kuala Krai	Tanah Merah
2000	1	1	-
2001	3	-	-
2002	6	-	-
2003	4	-	-
2004	8		1
2005	4	1	-
2006	7	-	-
2007	6	2	-
2008	16	8	1
2009	21	3	1
2010	15	4	1
2011	8	4	-
2012	17	5	3
2013	12	4	-
2014	18	4	-
2015	3	-	-

CHAPTER 5

CONCLUSION

5.1 Conclusion

In conclusion, the Kuala Krai regional climate model was mainly developed through the downscaling method based on RCP4.5. Although the reliability test indicated that RCP4.5 was slightly better, nevertheless, lack of significant difference in statistical test outcome resulted in need for future rainfall pattern under RCP8.5 as an alternative. Besides that, based on flood report, an Intensity-Duration-Frequency curve was drawn to indicate flood return period using Gumbel Distribution. Therefore, for the flood estimation, under RCP4.5, the precipitation that exceeding the flood threshold is 0.21% while probability of flood under RCP8.5 is 0.73%. At the same time, the rising in trend of the rainfall intensity in November indicates that there is higher flood potential around the end of year.

5.2 Recommendation for further study

This research focus on determines the potential flood disaster in the future with a deterministic model through the statistical downscaling. The main focus of the study is the flood estimation in Kelantan from 2021 until 2100 under both RCP4.5 and RCP8.5 through a model simulation. The model's highlight is the ability to perform the future rainfall intensity estimation with simplified equations that could reduce the data processing time.

For the model calibration, there are several initial data sources are required and their accuracy could directly affect the outcome reliability. The model is calibrated based on Kelantan rainfall station data in Peninsular Malaysia, coming with a future rainfall estimation, flood threshold analysis and future flood estimation.

It is recommended that other modelling software can be implemented to generate future rainfall model. Therefore, a comparison can be made among several models to determine the most reliable model that able to simulate future rainfall pattern in Kuala Krai.

References

- Adesina, A., 2020. Recent advances in the concrete industry to reduce its carbon dioxide emissions. *Environmental Challenges*, 1.
- Alam, A.S.A.F. et al., 2020. Agriculture insurance for disaster risk reduction: A case study of Malaysia. *International Journal of Disaster Risk Reduction*, 47.
- Araya, A. et al., 2020. Spatial analysis of the impact of climate change factors and adaptation strategies on productivity of wheat in Ethiopia. *Science of the Total Environment*, 731.
- Bachmir, S. et al., 2016. A quantitative analysis to objectively appraise drought indicators and model drought impacts. *Hydrology and Earth System Sciences*, 20, pp.2589–2609.
- Beguer á, S. et al., 2014. Standardized precipitation evapotranspiration index (SPEI) revisited: parameter fitting, evapotranspiration models, tools, datasets and drought monitoring. *International Journal of Climatology*, 34 (10), pp.3001–3023.
- Boe, J. et al., 2007. Statistical and dynamical downscaling of the Seine basin climate for hydro-meteorological studies. *International Journal of Climatology*, 27, pp.1643-1655.
- Brereton, R., G., 2019. The use and misuse of p values and related concepts. *Chemometrics and Intelligent Laboratory Systems*, 195.
- Brooks, N., 2003. *Vulnerability, Risk and Adaptation: A Conceptual Framework*. Tyndall Centre for Climate Change Research, 38.
- Carpenter, T.M., and Georgakakos, K.P., 2001. Assessment of Folsom Lake response to historical and potential future climate scenarios: 1. *Forecasting Journal of Hydrology*, 249 (4), pp.148-175.
- Dhuha, J. M. et al., 2021. Tropical seasonal changes impact on hematological parameters of goats. *Journal of the Indonesian Tropical Animal Agriculture*, 46(3), pp. 219-226.
- Edelmann, D. et al., 2021. On relationships between the Pearson and the distance correlation coefficients. *Statistics & Probability Letters*, 169.
- Erdeljić, V. et al., 2011. Distributed lags time series analysis versus linear correlation analysis (Pearson's r) in identifying the relationship between antipseudomonal antibiotic consumption and the susceptibility of *Pseudomonas aeruginosa* isolates in a single Intensive Care Unit of a tertiary hospital. *International Journal of Antimicrobial Agents*, 37(5), pp.467-471.
- Feyissa, G. et al., 2018. Downscaling of Future Temperature and Precipitation Extremes in Addis Ababa under Climate Change, *Climate*, 6(3), pp.58.
- Gao, C. et al., 2020. Effects of climate change on peak runoff and flood levels in Qu River Basin, East China. *Journal of Hydro-environment Research*, 28, pp.34-47.
- Grabowski, B., 2016. “ $P < 0.05$ ” Might Not Mean What You Think: American Statistical Association Clarifies P Values. *JNCI Journal of the National Cancer Institute*, 108(8).
- Gulacha, M. M. and Mulungu, D.M.M., 2017. Generation of climate change scenarios for precipitation and temperature at local scales using SDSM in Wami-Ruvu River Basin Tanzania. *Physics and Chemistry of the Earth*, pp.62-72.

- Gutmann, E.D. et al., 2012. A comparison of statistical and dynamical downscaling of winter precipitation over complex terrain, *Journal of Climate*, 25, pp.262-281.
- Hamid, T.H.T.A., 2018. Effect of 2014 massive flood on well water qualities: A case study on Kelantan River basin, Malaysia. *Journal of Water and Land Development*, 38(1), pp.127-136.
- Hammond, G.P. and Jones, C.I., 2008. Embodied energy and carbon in construction materials. *Energy*, 161(2), pp.87-98.
- Huang, Y.F. et al., 2016. Drought Forecasting using SPI and EDI under RCP-8.5 Climate Change Scenarios for Langat River Basin, Malaysia. *Procedia Engineering*, 154, pp.710-717.
- Hussain, A. and Ingole, B., 2020. Massive coral bleaching in the patchy reef of Grande Island, along the eastern Arabian Sea during the 2015/16 global bleaching event. *Regional Studies in Marine Science*, 39.
- Hussain, M., et al, 2017. Projected changes in temperature and precipitation in Sarawak state of Malaysia for selected CMIP5 climate scenarios. *International Journal of Sustainable Development and Planning*, 12(8), pp.1299-1311.
- Jebli, I. et al., Prediction of solar energy guided by Pearson correlation using machine learning. *Energy*, 224.
- Kang, S. et al., 2020. A review of black carbon in snow and ice and its impact on the cryosphere. *Earth-Science Reviews*, 210.
- Keenan, T.F. and Riley, W.J., 2018. Greening of the land surface in the world's cold regions consistent with recent warming. *Nature Climate Change*, 8, pp.825–828.
- Kotamarthi, V.R. et al., 2016. Use of Climate Information for Decision Making and Impacts Research: State of Our Understanding. Strategic Environmental Research and Development Program (SERDP) Project RC-2242, Technical Report, 54.
- Latif, S., and Mustafa, F., 2020. Bivariate joint distribution analysis of the flood characteristics under semiparametric copula distribution framework for the Kelantan River basin in Malaysia. *Journal of Ocean Engineering and Science*.
- Lund, A., and Lund, M., 2018. Partial Correlation using SPSS Statistics, Laerd Statistics, viewed 16 March 2021, < <https://statistics.laerd.com/spss-tutorials/partial-correlation-using-spss-statistics.php>>
- Marchini, M. et al., 2014. Impacts of genetic correlation on the independent evolution of body mass and skeletal size in mammals. *BMC Evolutionary Biology*, 14(1), pp.1-15.
- Maruti, S.F. et al, 2017. A hydrodynamic modelling of proposed dams in reducing flood hazard in Kelantan Catchment. *IOP Conference Series: Earth and Environmental Science*, 140, pp.1-8.
- Minhas, N.M. et al., 2020. Regression testing for large-scale embedded software development – Exploring the state of practice. *Information and Software Technology*, 120.

Ministry of Environment and Water 2021, *Rainfall data*, Department of Irrigation and Drainage (Kuala Lumpur), viewed 11 November 2021, <<https://publicinfobanjir.water.gov.my/hujan/data-hujan/?lang=en>>.

Nahm, F. S., 2017. What the P values really tell us. *Korean Journal of Pain*, 30(4), pp.241-242.

Nayan, N. et al, 2017. Flood Aftermath Impact on Business: A Case Study of Kuala Krai, Kelantan, Malaysia. *International Journal of Academic Research in Business and Social Sciences*, 7(6), pp.836-845.

Önen, F. and Bagatur, T., 2017. Prediction of Flood Frequency Factor for Gumbel Distribution Using Regression and GEP Model. *Arabian Journal for Science and Engineering*, 42, pp.3895-3906.

Rasel, M. M. and Islam, M. M., 2015. Generation of Rainfall Intensity-Duration-Frequency Relationship for North-Western Region in Bangladesh. *IOSR Journal of Environmental Science, Toxicology and Food Technology*, 9(9), pp.41-47.

Rasul, G., 2021. Twin challenges of COVID-19 pandemic and climate change for agriculture and food security in South Asia. *Environmental Challenges*, 2.

Robeva, R., Kirkwood, B. and Davies, R., 2013. Mechanisms of Gene Regulation: Boolean Network Models of the Lactose Operon in *Escherichia coli*. *Mathematical Concepts and Methods in Modern Biology*, pp.1-35.

Roux, R.L. et al., 2017. Comparison of statistical and dynamical downscaling results from the WRF model. *Environmental Modelling & Software*, 100, pp.67-73.

Royar-Carenzi, M. and Didier, G., 2019. Testing for correlation between traits under directional evolution. *Journal of Theoretical Biology*, 482.

Saha, P.P., Zeleke, K. and Hafeez, M., 2019. Impacts of land use and climate change on streamflow and water balance of two sub-catchments of the Murrumbidgee River in South Eastern Australia. *Extreme Hydrology and Climate Variability*, pp.175-190.

Samsurijan, M. et al., 2018. Land use change in Kelantan: Review of the Environmental Impact Assessment (EIA) reports. *Malaysian Journal of Society and Space*, pp.322-330.

Santos, M. and Fragoso, M., 2016. Precipitation thresholds for triggering floods in the Corgo Basin, Portugal. *Water* 2016, 8(9), pp.1-12.

Schweizer, V.J. et al., 2020. Integrated Climate-Change Assessment Scenarios and Carbon Dioxide Removal. *One Earth*, 3(2), pp.166-172.

Shamir, E. et al., 2019. Statistical and dynamical downscaling impact on projected hydrologic assessment in arid environment: A case study from Bill Williams River basin and Alamo Lake, Arizona. *Journal of Hydrology X*, 2.

Soh, Y.W. et al., 2018. Application of artificial intelligence models for the prediction of standardized precipitation evapotranspiration index (SPEI) at Langat River Basin, Malaysia. *Computers and Electronics in Agriculture*, 144, pp.164-173.

- Sohag, K. et al., 2015. Dynamics of energy use, technological innovation, economic growth and trade openness in Malaysia. *Energy*, 90 (2), pp.1457-1507.
- Sunyer, M.A., Madsen, H. and Ang, P.H., 2012. A comparison of different regional climate models and statistical downscaling methods for extreme rainfall estimation under climate change. *Atmospheric Research*. 103, pp.119-128.
- Tan, M, L. et al., 2020. SouthEast Asia HydrO-meteorological drought (SEA-HOT) framework: A case study in the Kelantan River Basin, Malaysia. *Atmospheric Research*, 246.
- Tukimat, N.N.A. et al., 2019. Projection the long-term ungauged rainfall using integrated Statistical Downscaling Model and Geographic Information System (SDSM-GIS) model. *Heliyon*, pp.1-8.
- Udin, W.S. and Malek, N.A., 2018. Flood risk analysis in Sg. Sam, Kuala Krai, Kelantan using remote sensing and GIS technique. *IOP Conference Series: Earth and Environmental Science*, 169, pp.1-9.
- UN, 2019. *World Population Prospects 2019. Comprehensive Tables (ST/ESA/SER.A/426)*, 1.
- Vishwanatha, J.S. et al., 2021. ANOVA studies and control factors effect analysis of cobalt based microwave clad. *Materials Today: Proceedings*.
- Xuan, W. et al., 2017. Evaluating historical simulations of CMIP5 GCMs for key climatic variables in Zhejiang Province, China. *Theoretical and Applied Climatology*, 128, pp.207–222.
- Yahara, N. S. et al., 2015. The December 2014 flood in Kelantan: A post-event perspective. *Warta Geologi*, 41, pp.54-57.
- Zhao, C. et al., 2017. Temperature increase reduces global yields of major crops in four independent estimates. *Proceedings of the National Academy of Sciences of the United States of America*, 114, pp.9326–9331.
- Zhao, T., Liu, D., and Li, Z., 2017. Correlated evolution of sternal keel length and ilium length in birds. *PeerJ*, 5(7), pp.1-11.
- Zheng, J. et al., 2019. Effect of equivalence ratio on combustion and emissions of a dual-fuel natural gas engine ignited with diesel. *Applied Thermal Engineering*, 146, pp.738-751.